Determination of 3'-phosphoadenosine-5'-phosphosulfate in cells using hydrophilic interaction liquid chromatography and mass spectrometry

Rua Dowood

Master's Thesis
Chemistry Department, Faculty of Mathematics and Natural Sciences
60 study points

UNIVERSITY OF OSLO

15.06.2016

Determination of 3'-phosphoadenosine-5'-phosphosulfate in cells using hydrophilic interaction liquid chromatography and mass spectrometry

Rua Dowood

Master's Thesis
Chemistry Department, Faculty of Mathematics and Natural Sciences
60 study points

UNIVERSITY OF OSLO

15.06.2016

2016

Determination of 3'-phosphoadenosine-5'-phosphosulfate in cells using hydrophilic interaction liquid chromatography and mass spectrometry

Rua Dowood

http://www.duo.uio.no/

Trykk: Reprosentralen, Universitetet i Oslo

Preface

The work presented in this thesis has been carried out at the Department of Chemistry, University of Oslo, in the Bioanalytics research group, in the period from January 2015 to May 2016. My supervisors have been Associate Professor Steven R. Wilson, Professor Elsa Lundanes and PhD candidate Elin Johansen.

For all the figures reproduced from other sources, the permission of use was applied for.

I would like to thank my supervisors for giving me an interesting and challenging project to work with and for all their help, advice and patience. I would especially like to thank Steven for his skilful guidance and encouraging comments throughout this study and for all the help and feedback while writing this thesis.

I would also like to thank all my fellow students and the employees at the group. A special thanks to Gosia for being a splendid officemate and for proofreading this thesis.

Thanks to Franziska for find time to proofread this thesis.

In addition, I would like to thank Professor Kristian Prydz and PhD candidate Ravi Adusumalli at the Section for Physiology and Cell Biology, Department of Biosciences, UiO for providing the internal standard and the samples. Thanks also for answering my questions regarding the pure biological aspects in this thesis.

Last but not least, a big thanks to my husband Moaeed and my daughters Yamame and Nasmah for making my life fantastic and having patience with me during my study.

Oslo, June 2016

Rua Dowood

Abstract

3'-Phosphoadenosine-5'-phosphosulfate (PAPS) is the universal donor of sulfate to sulfotransferases, a large group of enzymes that transfer sulfate to various molecules in the sulfation pathway. Methods that have been previously used to determine this important metabolite lack in specificity. The aim of the project was to develop a method for determining PAPS in cells and cellular fractions, using hydrophilic interaction liquid chromatography and mass spectrometry.

The developed method gave a retention time under 10 minutes, acceptable chromatographic efficiency and satisfactory repeatability in measurements. The method was able to separate PAPS from ATP and ADP, which could interfere with PAPS signal in the MS as they share mass spectrometric features. In addition, a simple sample preparation procedure was developed using ultra centrifugal filters. The method was evaluated regarding linearity, carry-over, within- and between-day precision etc., and PAPS levels was estimated in MDCK cell lines and their Golgi fractions, also following treatment with sodium chlorate (a PAPS synthesis inhibitor).

The combination of the ultra centrifugal filtration, as a sample preparation step, ZIC-*p*HILIC and ESI-MS detection was found to be a suitable technique for the analysis of PAPS.

Abbreviations

ACN	Acetonitrile
ADP	Adenosine diphosphate
ATP	Adenosine triphosphate
APCI	Atmospheric chemical ionization
APPI	Atmospheric photo ionization
CID	Collision induced dissociation
DC	Direct current
EIC	Extracted ion chromatogram
ESI	Electrospray ionization
ESI-MS	Electrospray ionization-mass spectrometry
H	Plate height
HILIC	Hydrophilic interaction liquid chromatography
HPLC	High performance liquid chromatography
ID	Inner diameter
IS	Internal standard
K_m	Michaelis-Menten constant
L	Length
LC	Liquid chromatography
LC-MS	Liquid chromatography-mass spectrometry
LC-UV	Liquid chromatography-ultraviolet
LLE	Liquid-liquid extraction
MALDI	Matrix assisted laser desorption ionization
MDCK	Madin-Darby canine kidney epithelial
MM	Molar mass
MP	Mobile phase
MS	Mass spectrometry
MS/MS	Tandem mass spectrometry
m/z	Mass-to-charge ratio
n	Number of replicates
N	Number of plates
NP	Normal phase

PAPS	3'-phosphoadenosine-5'-phosphosulfate[1]
PAPSTs	PAPS transporter proteins
PBS	Phosphate-buffered saline
PEEK	Polyether ether ketone
Q	Quadruple
QqQ	Triple quadruple
R %	Recovery %
rcf	Relative centrifugal force
RF	Radio frequency
RP	Reversed phase
RSD	Relative standard deviation
SD	Standard deviation
SDS	Sodium dodecyl sulfate
SDS-PAGE	SDS-polyacrylamide gel electrophoresis
SIM	Selected ion monitoring [1]
SRM	Selected reaction monitoring [1]
S/N	Signal to noise ratio
SP	Stationary phase
SPE	Solid phase extraction
STD	Standard solution
STs	Sulfotransferases
TIC	Total ion chromatogram
t_R	Retention time
Tris-HCl	Tris hydrochloride
UV	Ultraviolet
UV-vis	Ultraviolet – visible
$w_{0.5}$	Peak width at half height
ZIC	Zwitterionic chromatography
ZIC-*p*HILIC	ZIC-polymeric HILIC

[1] Sulfate is the spelling recommended by IUPAC, but sulphate is used in British English. Sulfate is used in this thesis even though British English is used elsewhere.

Table of content

1 Introduction

1.1 Sulfation pathway

Sulfation and sulfate conjugation (**Figure 1**) are important pathways in the metabolism of many drugs, other xenobiotics, neurotransmitters, and hormones [2], steroid biosynthesis, and facilitating the inactivation and elimination of potent endogenous chemicals including thyroid hormones, steroids and catechols [3]. The number of compounds which are sulfated is huge, yet the function of this pathway is not completely understood [3].

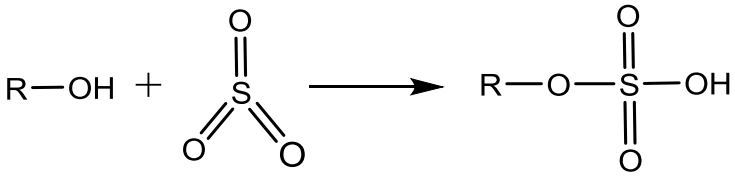

Figure 1: Sulfation reaction.

The sulfation pathway involves a sulfation reaction that is catalyzed by a large number of sulfotransferases (STs), which are enzymes that transfer the sulfuryl group ($-SO_3$) from a sulfate donor to the hydroxyls and primary amines of acceptors, and enable the hydrolysis of sulfate esters formed by the action of the STs [3]. The sulfation pathway is carried out in the secretory pathway, preferentially in the lumen of the Golgi apparatus, and in the cytoplasm (**Figure 2**). Sulfation in the Golgi lumen adds sulfate to tyrosine residues in proteins, glycans of proteoglycans (like heparin) and glycolipids. The sulfation of proteoglycans is important for the binding of growth factors to the cell surface receptors and their signalling, for immunological interactions, for formation of the extracellular matrix, and many more functions [4].

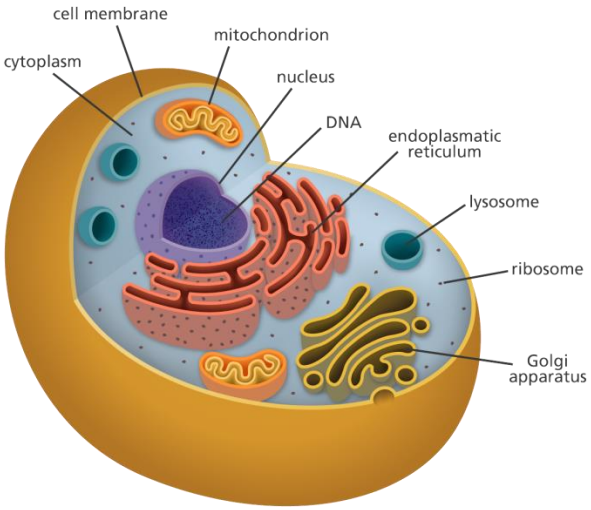

Figure 2: The structure of an animal cell. Reproduced from [5].

The nucleotide 3'-phosphoadenosine 5'-phosphosulfate[2] (PAPS) (**Figure 3 A**), which is also known as activated sulfate, is the sulfate donor in the sulfation reactions [2, 3, 6, 7].

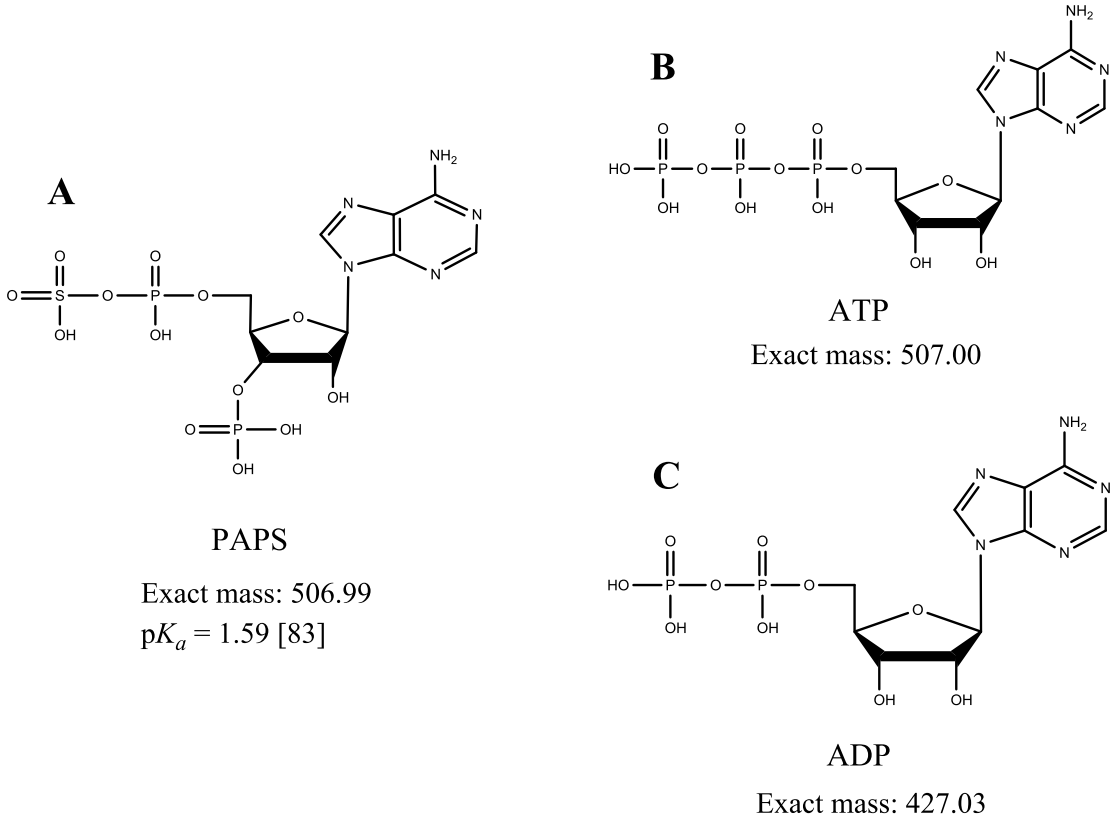

Figure 3: Molecular structures of 3'-phosphoadenosine 5'-phosphosulfate (PAPS), adenosine triphosphate (ATP) and adenosine diphosphate (ADP).

[2] IUPAC name: 6-Amino-9-[(2R,3R,4S,5R)-3-hydroxy-5-[(hydroxy-sulfooxy-phosphoryl)oxymethyl]-4-phosphonooxy-tetrahydrofuran-2-yl] purine.

1.2 PAPS

PAPS is synthesized in the cytoplasm in two sequential steps from inorganic sulfate and ATP (**Figure 3 B**) by a bifunctional PAPS synthase (PAPSS) [2, 8]. As seen in (**Figure 4**), inorganic sulfate combines with ATP to form adenosine 5'-phosphosulfate (APS) in the first step, and it is catalyzed by ATP-sulfurylase. APS reacts with another ATP in the second step, which is catalyzed by adenosine-phosphosulfate kinase, to form PAPS and ADP [9].

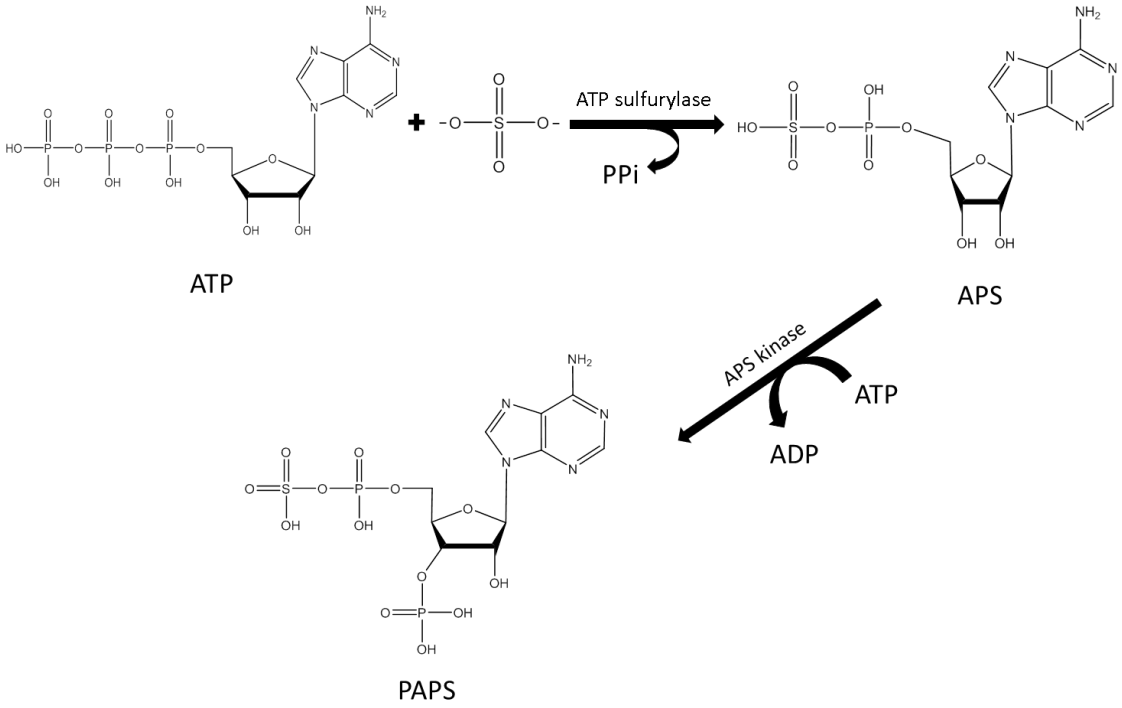

Figure 4: PAPS synthesis in a two-step reaction. Adapted from [9].

PAPS is transported into the lumen of the Golgi apparatus through Golgi membranes. This is mediated by PAPS-transporter proteins (PAPS-Ts), preferentially PAPS-T1, which are localized in the Golgi membrane (**Figure 5**) [4, 10]. PAPS-Ts are proteins that span the Golgi membrane several times to form a channel. It is thought that PAPS-T1 is pumping against a concentration gradient, thus the concentration of PAPS is proposed to be several times higher in the Golgi lumen than in the cytoplasm [11].

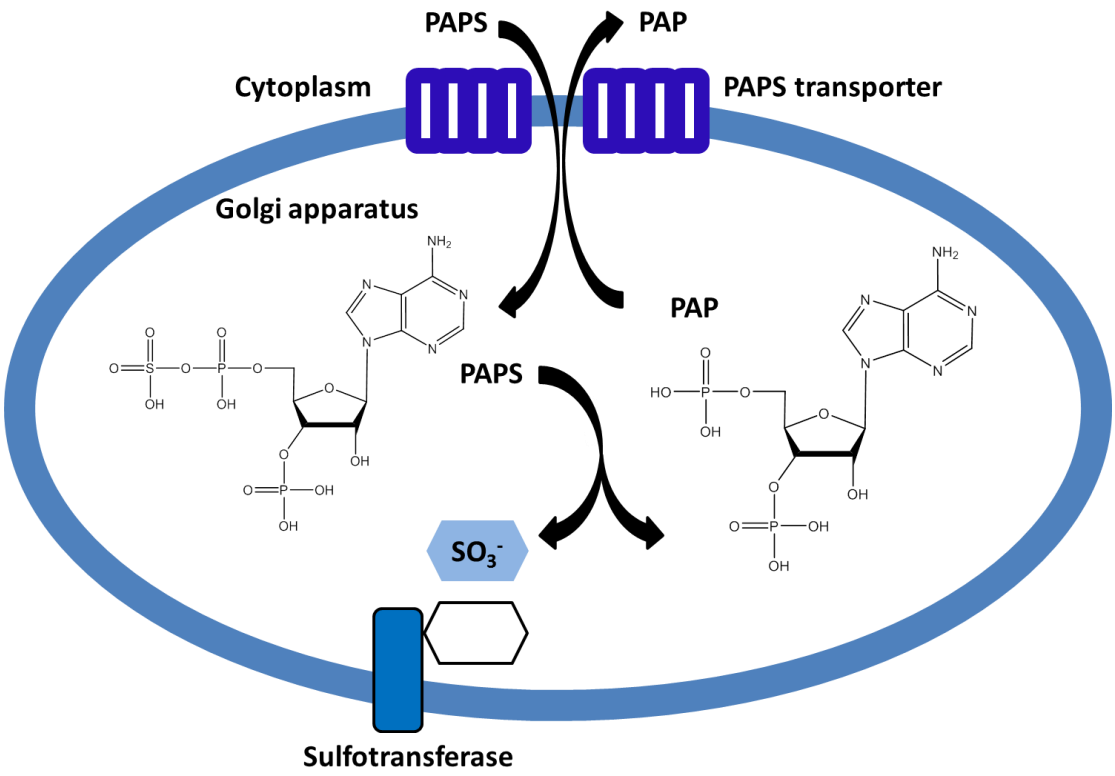

Figure 5: Schematic of the role of 3'-phosphoadenosine-5'-phosphosulfate in the sulfation pathway. PAPS transporters (PAPS-Ts) transport PAPS from the cytoplasm into the lumen of the Golgi apparatus. PAPS donates sulfuryl group to sulfotransferases STs and produces adenosine 3', 5'-diphosphate (PAP) as the result of a sulfotransferase reaction. Adapted from [12].

1.3 Determination of PAPS

Sulfation activities in cells depend on PAPS, as the sulfation reaction relies on the availability of this polar metabolite. PAPS concentrations have been estimated in different animal tissues and cellular systems with various assays. Isocratic reversed phase liquid chromatography (RPLC) employing a C30 column and UV detection was used to determine PAPS in hepatic cell extracts (0.42 nmol/10^6 cells) [13]. The determination of highly polar compounds such as PAPS by RPLC is challenging, as they require high concentrations of aqueous buffer in the mobile phase, which leads deficient peak shapes [14]. In addition, the UV detector does not provide highly selective identification and determinations [15, 16].

Ion-pair reversed-phase HPLC and UV detection was also used for determination of adenine nucleotides and nucleoside (including PAPS (0.55 nmol/mL plasma)) using triethylamine as a counter ion [17, 18]. Ion pair chromatography is arguably not a good option for the routine analysis because of mass spectrometry incompatibility of ion pairing reagents [19].

Indirect or radioisotope incorporation assays have been used to determine K_m[3] values for PAPS for a variety of sulfotransferases in a number of cellular systems (30-120 nmol/g liver, 0.8 nmol/10^6 cells) [7, 20-22]. In these assays, the formation of sulfo-conjugated substrates from radioisotope-labeled or fluorescent phenolic acceptors is measured [13]. Such methods are time consuming, and have limited selectivity since interferences or degradation products of the analyte may be detected in addition to the analyte [13]. Therefore, there is a need for more selective and reliable methods for quantification of PAPS concentrations in both whole cells and subcellular (Golgi) fractions.

1.4 Mass spectrometry

LC coupled to MS can be highly selective, and is a well suited tool for quantification and identification of many biological compounds [23]. The MS is composed of three basic components: an ion source, a mass analyzer, and a detector (**Figure 6**), which will be presented in more detail in the pages below. The analytes are evaporated and ionized (for non-pre-ionized analytes) in the ion source before entering the mass analyzer, where the ions are separated according to their mass-to-charge ratio (*m/z).* The separated ions are then passed to the detector to measure their abundances [24].

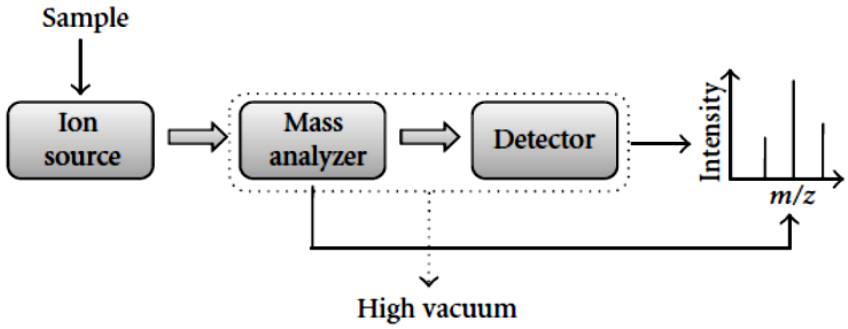

Figure 6: The basic components of the mass spectrometry. Reproduced from [24].

[3] K_m : Michaelis-Menten constant is an inverse measure of the strength of binding between the enzyme and its substrate.

1.4.1 Electrospray ionization

The ion source is the compartment where gas phase ions are produced and transferred to the second section of the instrument, the analyzer (**Figure 7**). There are many ionization techniques presently used with mass spectrometric instrumentations (i.e., ESI, APCI, APPI, ICP, MALDI) [25]. Electrospray (ESI) is the most common ionization source used in LC-MS, since it is highly suited for pre-ionized analytes and is a very "soft technique"; the ESI operates at atmospheric pressure with low transferred thermal energy, resulting in a low degree of fragmentation, allowing analysis of thermolabile compounds. ESI can easily be interfaced with LC and capillary electrophoresis separation techniques [24, 26].

In ESI, the analyte dissolved in a solvent is pumped (direct injection or LC), under atmospheric pressure, into the ionization source *via* a thin needle or a narrow-bore stainless steel capillary (~0.2 mm outer diameter and ~0.1 mm ID). An electrical potential (2–5 kV) is applied on the tip of the needle. At the capillary outlet and with the aid of a coaxial sheath gas (usually N_2) flow around the needle, a conical meniscus of accumulated charges is drawn out and deformed into a cone (Taylor cone) in the very high electric field [26, 27]. It splits into a fine aerosol of charged droplets, which move towards an opposite charged electrode (**Figure 7**).

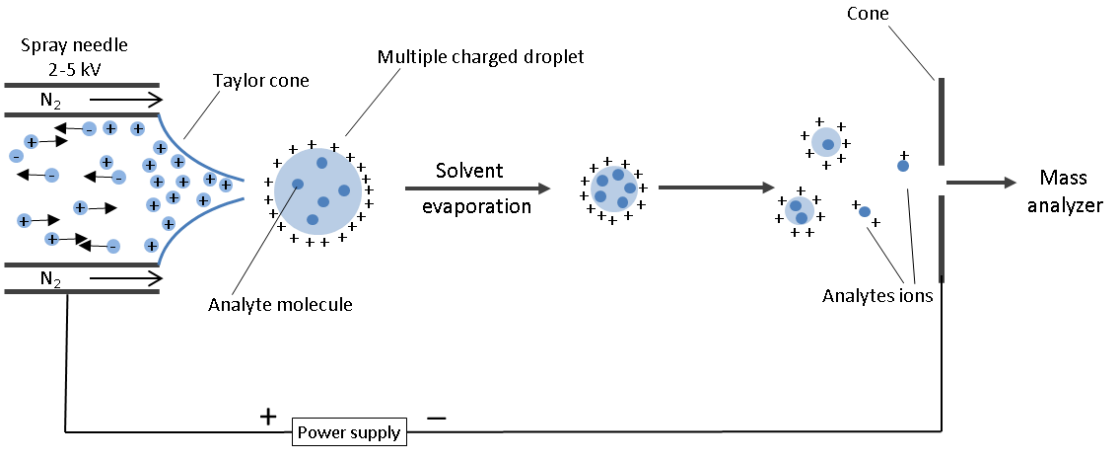

Figure 7: Representation of the electrospray ionization process. By applying high voltage, a Taylor cone (a drawn-out meniscus with an excess of charge) is formed and split into charged droplets. The droplets evaporate while they move towards the opposite charged electrode. As the repulsion in the droplets is increased, free gaseous ions are ejected. Adapted from [28].

Then, as the solvent evaporates, the repulsive forces of the ions inside the droplet increase due to a surplus of similar charges in the droplet. Once the repulsive forces exceed the surface tension, the droplets undergo fission to create smaller droplets. Several cycles of evaporation of the solvent and fission of the droplets result in the ejection of gaseous ions from the droplet remains that are driven electrically towards the entrance of the mass analyzer through a sampling cone (kept in the interface of atmospheric pressure and the high vacuum), which is typically placed at 1–3 cm from the spray needle tip [19, 26, 29].

1.4.2 Mass analyzer

There are several types of mass analyzers available, for example magnetic or electric sector mass analyzer, quadrupole, ion trap (linear and three-dimensional), orbitrap, time-of-light (TOF), and Fourier transform ion cyclotron resonance (FT-ICR). The separation and isolation of ions in the mass analyzer are influenced by an electrical or magnetic field [24, 25]. The choice of the mass analyzer depends on the price, resolution, mass range, scan rate, detection limits and the ability to perform tandem MS [25]. Single and triple quadrupoles have been used as mass analyzer during the study, and will be focused upon here.

1.4.3 Quadrupole mass analyzer

The quadrupole is the most commonly used mass analyzer in laboratories as it is relativity inexpensive, small in size, robust and easy to maintain [25]. A single quadrupole mass analyzer consists of four parallel rods that are connected electrically (**Figure 8**). An oscillating electrical field is created when a certain direct current (DC) and a radio frequency (RF) is applied on one of the pairs and the opposite DC and RF on the other pair. The ions formed in the ion source start to oscillate between the rods in the x- and y- direction when they enter this field in the z-direction [19, 30]. Ions with stable oscillation will not collide with the quadrupole and will reach the detector, while ions with non-stable oscillation will collide with one of the rods, neutralize and will not be detected. By varying the values of the applied DC and RF between the rods, the stability of the oscillation of ions can be controlled. Only ions with specific *m/z* ratios will pass the path toward the detector at certain DC and RF values [25].

There they are detected in several ways e.g. the using a Faraday cup or other electron multiplier. In a Faraday cup, briefly, the ions are neutralized and a current is created and measured [24].

In this project (targeting only a few compounds), selected ion monitoring (SIM) was used. In SIM, selected *m/z* values are recorded by fine-tuning and keeping DC and RF values constant (as opposed to scanning a range of masses, which can reduce sensitivity [31, 32]).

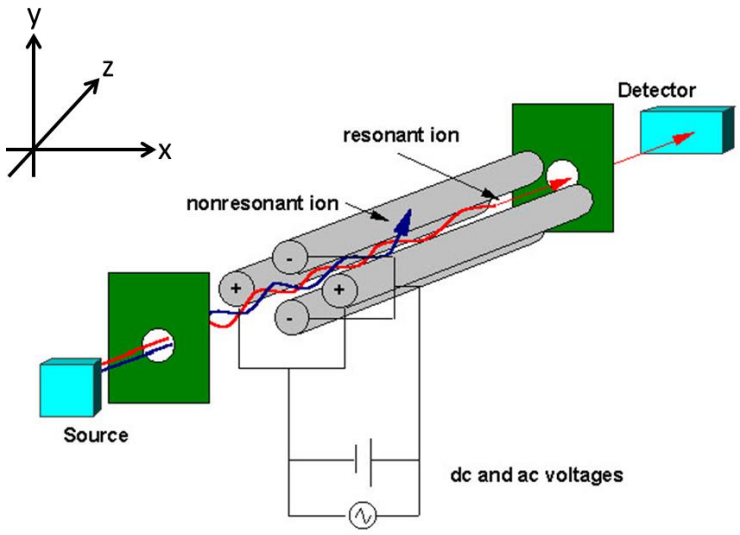

Figure 8: Schematic of a triple quadrupole mass analyzer with four parallel rods that are connected electrically. For given DC and AC voltages, only ions of a certain *m/z* will oscillate in a stable path and reach the detector and all other ions will collide with one of the rods. Reproduced from [33] with elements added by the author of the thesis.

1.4.4 Tandem MS

SIM can be expanded to a tandem MS (MS/MS) experiment. In MS/MS, usually two or more mass analyzers in a single instrument are employed for increasing sensitivity and selectivity. Many possible combinations of mass analyzers in MSMS are available: triple quadrupole (QqQ), quadrupole-TOF (Q-TOF), Ion trap – TOF (IT-TOF), LIT – Orbitrap and LIT – FT-ICR. The principle of tandem MS is the isolation of a selected *m/z* (precursor ion), followed by a fragmentation of this ion, and selection/detection of the selected fragments (product ions) (**Figure 9)**. Due to its low cost and ease of use, the triple quadrupole is the most commonly used mass spectrometer for MS/MS [25].

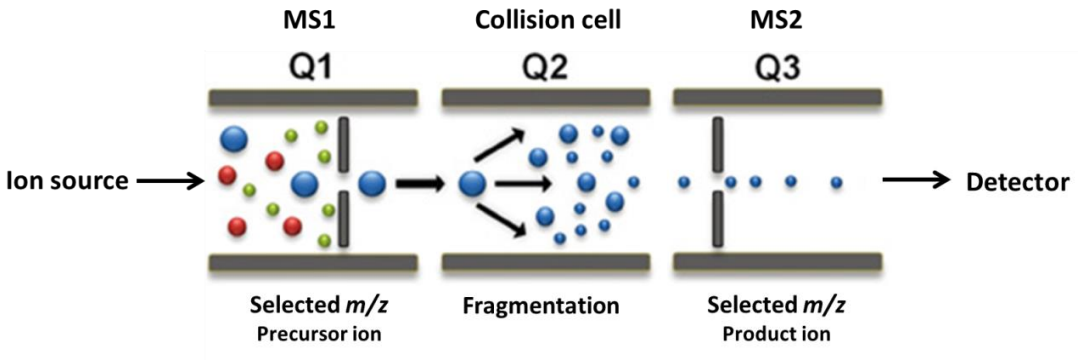

Figure 9: Schematic of a triple quadrupole mass analyzer. The precursor ion is selected in Q1 and collided with neutral molecules (for fragmenting) in Q2. Product ions are selected in Q3 before being detected. Reproduced from [34] with elements added by the author of the thesis.

The triple quadrupole is arguably the most used mass analyzer for quantitative purposes. It consists of three sets of quadrupole filters. The first and third (Q1 and Q3) quadrupole function as mass analyzers, and the second one (Q2) as a collision cell, as it is shown in **Figure 9**. Many scan modes can be applied e.g. product ion scanning and selected/multiple reaction monitoring (SRM/MRM). The first quadrupole (Q1), acting as a mass filter, allows a selected *m/z* (precursor ion) to enter the collision cell (Q2). In Q2, the ions (precursor ion) are accelerated by electrical potential to high kinetic energy, collide with neutral gas molecules (He, N_2 or Ar) and fragment into product ions by collision-induced dissociation (CID). The product ion with a specific *m/z* is allowed to pass through (Q3) and is detected. In this way, only specific precursor ions with specific product ions are detected.

Although MS and MS/MS are very powerful, the presence of a wide range of (polar and non-polar) molecules in the sample matrix can lead to ion suppression (the impact of the less volatile compounds in the sample matrix and interfering compounds on the signal of the analyte of interest through reducing the efficiency of droplet formation and/or evaporation [35, 36]). Ion suppression may have an effect on the method performances such as detection capability, repeatability and accuracy [35]. Another challenge is if compounds are isomers (sharing the same mass and perhaps product ions). Separation of compounds prior to MS (using e.g. LC) may be mandatory in these matters.

1.5 Liquid chromatography

An LC system typically consists of a pump, an injector, a column and a detector unit. The sample is introduced to the system and transported with a mobile phase (MP) through the column that contains a stationary phase (SP). Different degrees of interactions between the sample components and the stationary phase lead to different migration rates through the column, resulting in a separation [19]. The stationary phase is typically bound to small particles.

LC was introduced in 1906 by Mikhail Tswett [19]. Martin and Synge found in 1941 that the separation efficiency could be improved by using separation columns filled with very small particles [37]. Later, LC also became referred to as high pressure liquid chromatography or high performance liquid chromatography (HPLC) and lately as ultra high performance liquid chromatography (UHPLC) [19]. LC has become one of the most used analytical/separation techniques [38].

Particle-packed columns are currently the most used columns (compared to e.g. open tubular and monolithic columns), and are commercially available in various functionalities and dimensions (**Table 1**).

Table 1: Dimensions and flow rates in HPLC particle packed columns. Adapted from [19].

Column type	ID (mm)	L (cm)	d_p (µm)	Typical flow (µL/min)
Conventional	2-5	3-25	3-5	100-2000
UHPLC	1-2	3-15	1.7-1.9	100-1000
Micro-bore	0.5-1	3-25	3-5	20-100
Capillary	0.1-0.5	3-25	3-5	1-20

Silica-based columns are most common. However, mobile phases with high pH (> 8) cause early degradation for silica-based columns due to silica support dissolution [39]. Hence, there are limitations of the utility of silica-based columns for high pH applications [40]. Organic polymer based columns can be a good alternative in this case, as they are stable over a wide pH range [14, 41]. The column diameter can also be varied; using more narrow columns can provide higher sensitivity, but may require dedicated pumps for handling low flow rates used with such columns.

The column efficiency indicates the performance of the column in terms of the retention time/peak width relation [42]. It is a presentation of the extent of band broadening a compound undergoes during chromatography when a Gaussian distribution is assumed for each band [19]. The plate number (N) or the plate height (H) represent the column efficiency and they are measured by the equations 1 and 2, where L is the column length, t_R is the retention time of the analyte and $w_{0.5}$ is the peak width at half peak height.

$$N = 5.54\,(t_R/w_{0.5})^2 \qquad \text{(Equation 1)}$$

$$H = L/N \qquad \text{(Equation 2)}$$

A column with high efficiency has a large plate number and small plate height. To improve the efficiency of a column, the plate number can be increased by increasing the column length and/or reducing the plate height. For particle packed columns, H can be reduced by reducing the particle diameter (d_p) as described in Van Deemter equation (Equation 3) [19].

$$H = A + B/u + Cu = 2\lambda d_p + 2\gamma D_M/u + f(k){d_p}^2 u/D_M \qquad \text{(Equation 3)}$$

Where A, B and C are constants related to eddy dispersion, longitudinal diffusion and mass transfer in the mobile and stationary phases, respectively, u is the linear velocity, λ is the structure factor of the packing material, d_p is the particle diameter, γ is the obstruction factor, k is the retention factor and D_M is the diffusion coefficient of the analyte in the MP.

The disadvantage of increasing the length of the column is an increase in the analysis time and the back pressure. A column with smaller particles will also produce higher back pressure [19]. In addition, not all stationary phases are available on small particles.

1.5.1 Separation modes in LC

The chromatographic separation modes (principles) in LC depend on the interactions between the SP, the analyte and the MP, and are based mainly on the type of the stationary phase [38]. Several principles are available, but the most known are adsorption/normal phase liquid chromatography (NPLC), reversed phase liquid chromatography (RPLC), ion pair chromatography, ion exchange chromatography, exclusion chromatography and hydrophilic interaction liquid chromatography (HILIC).

RPLC is the most used principle, it currently represents 70 % of LC separations [43]. A nonpolar stationary phase of hydrocarbon surface functions (C8, C18, etc.) attached to silica based materials or organic polymers based materials (e.g. poly (styrene-co-divinyl benzene)), and a buffered polar mobile phase consisting of water and miscible solvents (methanol, acetonitrile) are used. The separation in RP is based on the hydrophobicity (lipophilicity) of the analytes [44]. The more hydrophobic analytes are more retained on the nonpolar SP than less hydrophobic analytes. As a consequence, RPLC is not well suited as a separation mode for very polar analytes such as PAPS. Polar compounds are not or insufficiently retained on RPLC columns as they typically elute in the void volume of the column [43].

NPLC or adsorption chromatography is used for the separation of compounds with substituents of different polarity. It is a suitable separation principle for mixtures containing positional isomers [45]. A polar material with specific surface area such as silica, bonded silica (diol, cyano. etc.) and alumina is used as stationary phase [45, 46]. An organic relatively nonpolar mobile phase, typically hexane, elutes the compound according to their polarity. The nonpolar compounds are eluted before the polar compounds that are strongly adsorbed to the polar SP. NPLC has been used as a separation principle for polar and hydrophilic compounds over a long period. However, the expensive, toxic, and environmentally unfriendly organic mobile phases minimize the usage of NPLC [43]. In addition, it is problematic to dissolve polar analytes in these nonpolar MPs [43].

The separation by ion-exchange chromatography (IEX) is based on the charge characteristics [47]. The ionic groups in the stationary phase (ion exchanger) interact electrostatically with the oppositely charged groups on the analyte [47]. IEX is a suitable separation tool for compounds containing ionic or ionizable groups such as amino acids, ionic metabolic products and organic ions. The mobile phase is water with salts/buffer to regulate the pH and the ionic strength, and the stationary phase possesses ionic groups (SO_3^-, NR_3^+) covalently bound to a non-soluble matrix [19]. IEX is incompatible with ESI-MS due to the high salt concentrations in the employed MP that reduce the sensitivity of MS [48].

HILIC is an interesting alternative for the determination of very polar compounds [43, 49], and combines many of the features of the above-mentioned principles, and will be described in detail.

1.6 Hydrophilic interaction liquid chromatography

HILIC was introduced in 1990 by Alpert as an alternative LC mode for separating polar and hydrophilic compounds on polar stationary phases [50]. HILIC has a wide range of separation options, since it combines the characteristics of other separation principles by employing a polar stationary phase similar to NPLC, and a mobile phase consisting of water and organic solvent like RPLC. It also has the ability to separate charged analytes as in ion chromatography [51].
Primarily, HILIC was used for the determination of amino acids, carbohydrates and peptides [49]. Lately, it has been successfully applied for determination of polar drugs, metabolites, nucleotides, pharmaceuticals and many neutral and charged compounds in proteomics and glycomics [49, 51-53].

1.6.1 Separation mechanisms in HILIC

The retention mechanisms in HILIC are still under discussion, and depend on the type of the SP, composition of the MP and the chemical properties and the structure of the analytes. The mechanisms are a complicated and multi-modal combination of many mechanisms, but three essential retention mechanisms can explain the separation of polar compounds in HILIC columns: liquid-liquid partitioning, adsorption and electrostatic interactions [14].

Partitioning is the most accepted separation mechanism in HILIC [14]. Water molecules are attracted by the polar functional groups on the surface of the SP to create a water-enriched layer on the surface of the stationary phase. This layer works like a stagnant liquid stationary phase (**Figure 10**). Based on their polarity and solvation, the analytes dissolved in the MP will partition between the water layer stationary phase and the high organic content mobile phase. The solvation in the water layer typically increases with the polarity of the analytes, thus increasing the retention [14, 51, 54].

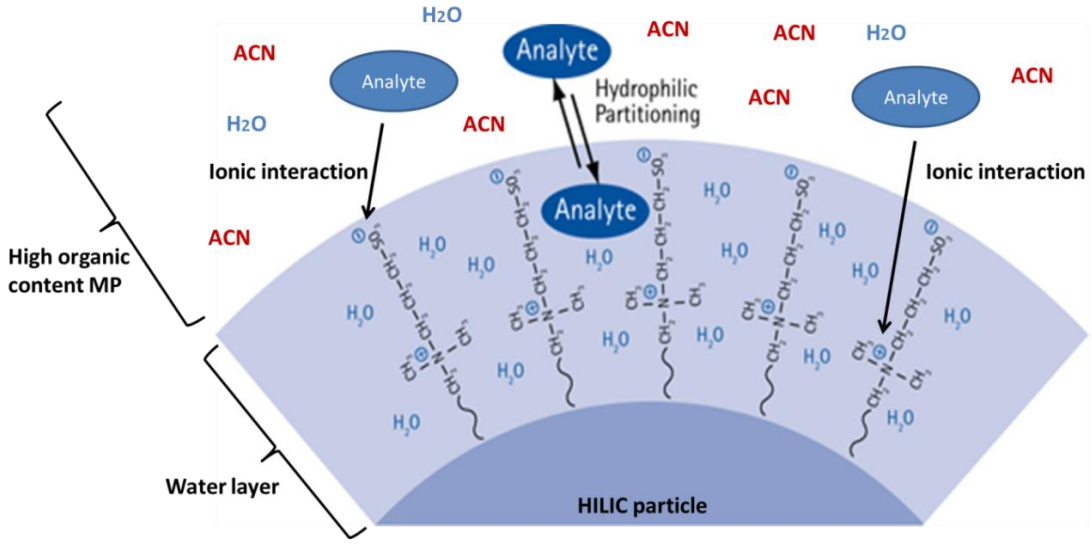

Figure 10: Establishing of the water-enriched layer on the surface of a zwitterionic stationary phase in HILIC columns. Reproduced from [55] with elements added by the author of the thesis.

Like in NPLC, adsorption is competition between the analytes and the MP for polar adsorption sites on the surface of the SP (adsorbent) [51, 56]. Electrostatic interactions (ion-exchange or ion repulsion) between the ionized analyte and the ionic functional groups in the SP play an important role in HILIC retention mechanisms [14, 49, 57].

Additional retention mechanisms such as dipole-dipole interactions between the non-ionized polar analyte and the functional groups in the SP and hydrogen bonding enhance the retention in combination with ionic interactions, adsorption and partitioning [14, 50, 53, 57].

1.6.2 Stationary phases

Stationary phases in HILIC are polar, and could be e.g. non-modified silica (bare particles), or polar functional groups attached to silica-particles; such as amine, amide, cyano, diol, polyethylene glycol, cyclodextrine and other polar monomeric and polymeric functional groups [49, 51]. The stationary phases can be neutral, anionic, cationic or zwittierionic.

Retention on bare silica is caused by partitioning and adsorption at low pH, and ion exchange at higher pH. Silanol groups are negatively charged at higher pH, and this will increase the retention of cationic analytes. Bare silica SP is used mainly in pharmaceutical analysis [49, 58].

Silica-based chemically bonded stationary phases have been used in a wide range of application. For example, diol-silica bonded phases have been applied for protein separations, amino and amide-silica phases are used for separation of sugars, amino acids and peptides [49, 51, 59].

Polymer-based stationary phases are usually modified with ion-exchange or zwitterionic functional groups [49]. Compared with silica-based stationary phases, they are not widely used in HILIC due to lower separation efficiency. However, polymeric columns have the advantage at very low pH or very high pH separation conditions, where silica-based columns are not stable [14, 41, 60].

In addition to particle packed columns, monolithic stationary phases are also used in HILIC separation. There are two types of monolithic columns, silica-based and organic polymer. They provide fast separations due to the high permeability in the monolithic structure that allows using of high flow rates without increasing column back pressure [14, 49]. However, these columns are not widely available.

1.6.3 Zwitterionic HILIC

ZIC-HILIC is used for the separation of ionic and ionizable species on a zwitterionic stationary phase. The ZIC-HILIC stationary phase involves zwitterionic functional groups such as phosphorylcholine (ZIC-cHILIC) and sulfobetaine attached to porous silica particles (ZIC-HILIC) or porous polymer particles (ZIC-*p*HILIC) (**Figure 11**) [61].

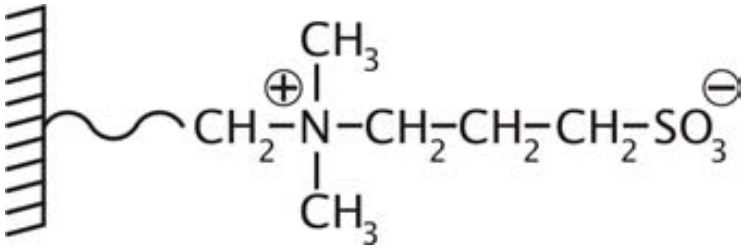

Figure 11: Schematic illustration of the ZIC-HILIC stationary phase (3-sulfopropyldimethylalkylammonio inner salt). Reproduced from [62].

Figure 11 shows the structure of the functional group in zwitterionic sulfoalkylbetaine stationary phase. Anion-exchange and cation-exchange interactions are assumed to take place. The separation is based on the ability of the positively and negatively charged analytes to access both the fixed positive quaternary ammonium group and negative sulfonic acid group. It is believed that the easily accessible sulfonic acid groups repulse negatively charged analytes, but the more shielded quaternary ammonium groups do not repulse positively charged analytes as strongly [49, 51, 63, 64]. This bonded stationary phase can adsorb water molecules by hydrogen bonding to create the water layer that would control the retention. The separation in ZIC-HILIC columns is also achieved by partitioning of the analytes between the MP and the water layer in the surface of the SP, and by weak electrostatic interactions between the analytes and charged functional groups on the surface of the SP [49, 51, 64]. The weak electrostatic interactions allow using of low buffer concentrations in the MP, which is an advantage in MS detection to avoid suppression of MS signal [61].

ZIC-*p*HILIC has been successfully used for separation of nucleoside triphosphates (e.g. ATP), which are very polar compounds and have poor retention on reversed phase columns with conventional mobile phases [65].

1.6.4 Mobile phase

Common mobile phases used in HILIC consist of water and water-miscible organic solvents [49]. It is possible to carry out the separation in HILIC in isocratic or gradient mode. A high percentage of organic solvent (50-90 %) is used in the isocratic mode, while the gradient mode starts with a high percentage of organic solvent and ends with a higher percentage of water to increase the elution strength during the separation [14, 50].

The retention in HILIC is influenced strongly by the polarity of the organic solvent, as the elution strength of the organic solvents increase with their polarity: water > methanol > ethanol > acetonitrile > acetone [51]. Acetonitrile (ACN) is the most used organic solvent in HILIC due to its moderate elution strength that gives acceptable retention times because its chemical structure eliminates formation of hydrogen bonds. ACN has low viscosity which results in efficient separation at low back pressure [14, 54].

The content of 5-40 % water in the mobile phase ensures the formation of a water layer on the surface of the SP and a reasonable retention time for very hydrophilic analytes [50, 51]. More than 50 % water in the mobile phase is not recommended in HILIC because then the separation tends to be ion-exchanging. The high organic content (60-95 %) in the MP is an advantage when MS is used, because of the high efficiency of spraying and desolvation that enhances the sensitivity of the MS [66].

Ionic additives (buffers or acids) are also essential in the HILIC mobile phase to control the pH and the ionic strength. As the pH and ionic strength of the MP have a considerable effect on the retention and separation selectivity of ionic and ionizable analytes, they have to be selected carefully. The ionization of analytes and the polar groups in the SP could be increased or reduced by adjusting the pH according to their pK_a. Thus, enhancing or suppression of the electrostatic interactions may occur [14, 49, 54]. Ammonium salts are usually used in HILIC-MS due to their solubility in MPs with high organic content and their volatility [51].

1.7 Sample preparation

The sample preparation is an essential step in most analytical techniques to eliminate the effect of the matrix of the biological samples (interferences and destructive components) and to enrich the analyte of interest prior to the quantification [19]. Removal of proteins and other high molar mass molecules is often the main purpose of the sample preparation, as they are responsible for the most of back pressure and declining column performance problems [67].

Liquid-liquid extraction (LLE), solid phase extraction (SPE) and protein precipitation are the most used techniques for preparing samples [19]. The typical solvents used in LLE are non-polar organic, therefore polar analytes (e.g. PAPS) in the sample (aqueous phase) may not be extracted into the organic phase. Other drawbacks by LLE are time consumption, large consumption of organic solvent and emulsion formation [19, 68]. SPE is relatively expensive [68]. Protein precipitation include several steps for forming and isolating the precipitate [69]

Centrifugal ultrafiltration (**Figure 12**) is a rapid and simple sample preparation procedure used to isolate the analyte of interest from the sample matrix by employing centrifugal filter devices. Low molecular weight components (e.g. PAPS) can be separated from high molar mass components (e.g. proteins) by centrifugal ultrafiltrating the sample through a membrane with an appropriate molar mass cut-off [67].

In addition to the short operation time and ease of use, this technique offers satisfactory recovery and reproducibility, requires low sample volume (< 100 µL) and does not need protein precipitation prior to filtration for the cell lysate matrix [70-73].

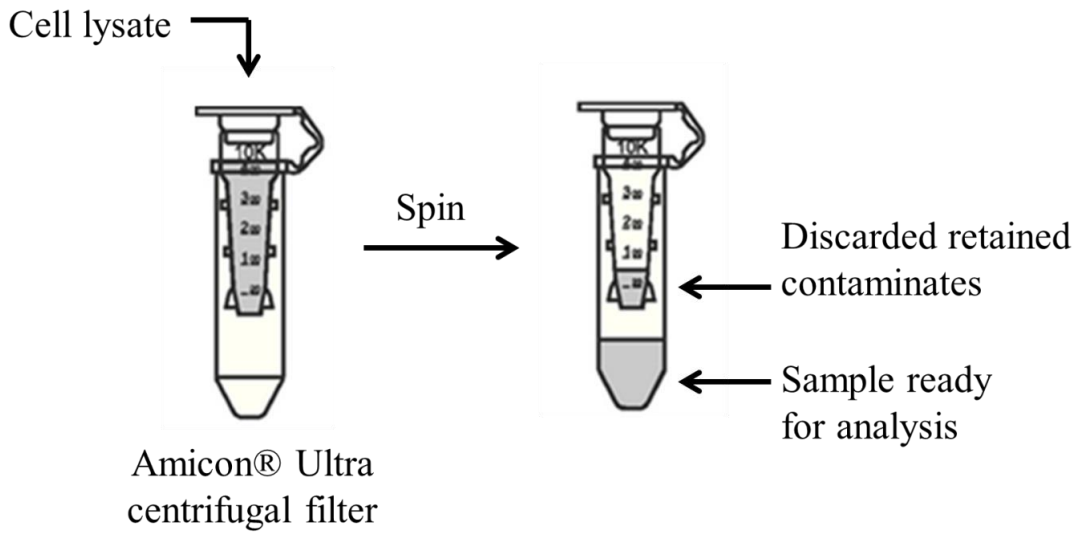

Figure 12: Centrifugal ultrafiltration of cell lysate in Amicon® Ultra centrifugal filters. The figures of the filters were reproduced from [74].

1.8 Aim of study

The aim of this study was to develop and evaluate a simple, sensitive and selective method for determination of PAPS in cells and subcellular fractions.

From the above, it is hypothesized that centrifugal ultrafiltration, ZIC-*p*HILIC, ESI and quadruple MS are appropriate techniques for the aim. The developed method was to be applied for whole cells and subcellular (Golgi) fractions.

2 Experimental

2.1 Chemicals

Type 1 water (resistivity (MΩ•cm @ 25 °C) >18.0 [75]) was from a Milli-Q ultrapure water purification system (Millipore, Bedford, MA, USA). HPLC grade ACN, acetic acid and methanol were from VWR (Radnor, PE, USA). Ammonium carbonate ($(NH_4)_2CO_3$), was from Fluka (Buchs, Switzerland). PAPS (adenosine 3′-phosphate 5′-phosphosulfate lithium salt hydrate), ATP (adenosine 5′-triphosphate disodium salt hydrate, ≥99%) and ADP (adenosine 5′-diphosphate, ≥95%) were from Sigma-Aldrich (St. Louis, MO, USA) (purity ≥60%) [76]. Nitrogen (99.96 %) was from AGA (Oslo, Norway). The internal standard (^{13}C-PAPS ($^{13}C_{10}H_{15}N_5O_{13}P_2S$)) was from Section for Physiology and Cell Biology, Department of Biosciences UiO (Oslo, Norway); for synthesis procedure, see section **6.1** in appendix and [77, 78]. Sodium chloride for analysis was from Merk (Darmstadt, Germany).

Bromophenol blue, Coomassie Brilliant Blue (R-250), dithiothreitol (DTT), glycerol and sodium dodecyl sulfate (SDS) were from Sigma-Aldrich. PageRuler™ Prestained Protein Ladder (10-180 kDa) and 20X NuPAGE® MOPS SDS running buffer were from Thermo Fisher Scientific (Waltham, MA, USA). 1M Tris-HCl pH 7.0 was from Oslo University Hospital (Oslo, Norway).

2.2 Consumables

Amicon® Ultra 0.5 mL centrifugal filters with a 10K cut-off were from Merck Millipore (Billericia, MA, USA) [79]. Eppendorf® Safe-Lock microcentrifuge tubes (1.5 mL) and Microvials PP (0.3 mL) with snap ring were from VWR. Pipettes (Finnpipette®F2) 5-40, 20-200, 100-1000 µL and 1-5 mL were from Thermo Scientific. NuPAGE®Novex® 12% Bis-Tris protein gels were from Thermo Fisher Scientific.

2.3 Units for sample storage and sample preparation

A NanoDrop™ 2000 UV-Vis spectrophotometer was from Thermo Scientific. A Centrifuge 5415 R was from Eppendorf (Hamburg, Germany). A Speed-vac™ concentrator (SC110) was from Savant (Hicksville, NY, US). An ultrasonic cleaner (Branson 2510) was from Bransonic® (Bloomfield, USA). One freezer (-80 °C) was from Arctiko (Esbjerg, Danmark) while one freezer (-18 °C) was from Husqvarna (Stockholm, Sweden) and the refrigerator (+4 °C) was from Bosch (Gerlingen, Germany).

2.4 Samples

The cell pellets (MDCK I, MDCK II and MDCKB22) and Golgi fractions samples were provided by Ravi Adusumalli (PhD student at the Section for Physiology and Cell Biology, Department of Biosciences, UiO). For cell culturing and preparation, see section **6.2** in appendix.

2.5 Solutions

In initial stages of the study, a stock solution of PAPS was prepared by dissolving the purchased 1 mg of PAPS in a mixture of ACN and type 1 water in the ratio 50/50 (v/v) to a final concentration of 200 µg/mL. When the final conditions of the method were established, a more convenient stock solution used in the main part of the study was made by dissolving the purchased 5 mg of PAPS standard in a mixture of ACN and type 1 water (65/35, v/v) to a final concentration of 1 mg/mL. The stock solution of the internal standard (IS) was prepared by diluting a 1 mL of 1 mg/mL with a mixture of ACN and type 1 water (65/35, v/v) to 10 mL to a final concentration of 100 µg/mL. All stock solutions were divided in small aliquots which were frozen (-80 ºC).

Working solutions of PAPS and the internal standard were prepared daily by diluting the stock solutions in the mobile phase or in the desired mixture of ACN and 100 mM ammonium carbonate solution.

Stock solutions of ATP and ADP were prepared by dissolving 1 g of each in 10 mL of the MP to a final concentration of 100 mg/mL. These solutions were divided in small

aliquots which were frozen (-18 ºC). Working solutions were prepared by diluting the stock solutions with the MP to the desired concentrations.

A solution of 0.5 M NaCl was prepared by dissolving 14.61 g of NaCl in 500 mL type 1 water. The solution was stored at 4 ºC. A 100 mM ammonium carbonate solution was prepared by dissolving 4.80 g of ammonium carbonate in 500 mL type 1 water. The solution was stored at 4 ºC.

A 10 % (w/v) SDS solution was prepared by dissolving 10 g of SDS in 100 mL type 1 water. A 1.0 % (w/v) bromophenol blue solution was made by dissolving 1 g of bromophenol blue in 100 mL type 1 water, while 0.1 M DDT was prepared by diluting 1 mL of 1 M DDT with type 1 water to 10 mL. A 0.5 M Tris-HCl pH 7.0 solution was prepared by diluting 5 mL of 1 M Tris-HCl pH 7.0 with type 1 water to 10 mL.

To prepare 100 mL of 1X SDS sample loading-buffer (1% (w/v) SDS, 1 mM DTT, 20 % (v/v) glycerol, 20 mM Tris-HCl pH 7.0 and 0.01 % (w/v) bromophenol blue), 4 mL of 0.5 M Tris-HCl, 20 mL of glycerol, 10 mL of 10 % (w/v) SDS, 1 mL of 1.0 % (w/v) bromophenol blue, 1 mL of 0.1 M DDT, and 64 mL type 1 water were mixed. To prepare 100 mL of Coomassie Blue Staining solution (10% (v/v) acetic acid, 0.005 % (w/v) Coomassie Brilliant Blue and 90% (v/v) water) was done by dissolving 5 mg of Coomassie Brilliant Blue (R-250) in a mixture of 10 mL acetic acid and 90 mL type 1 water.

Method evaluation solutions were prepared by spiking 50 µL of cell lysate samples (1×10^5 cells) with standard solutions to a concentration of 2, 10, 100 and 200 µg/mL (in addition to endogenous levels) and with internal standard to a concentration of 10 µg/mL (**Table 2**).

Table 2: Concentration of PAPS and IS in validation solutions.

Validation solution	PAPS (µg/mL)	IS (µg/mL)
Low	2	10
Medium	10	10
High	100	10
Very high	200	10

2.6 Sample preparation

2.6.1 Cell lysis

Ultra-sonication

In the ultra-sonication method, lysing was carried out by adding 100 µL of an aqueous solution (type 1 water and 100 mM ammonium carbonate (50/50, v/v)) to the cell pellets (12 x 10^6 cells) and placing the mixture in an ultrasonic bath with cooling periods (10 sec in the bath and 10 sec on ice, six cycles) to disrupt cell membranes and release polar biological molecules (such as PAPS). Then the cells were centrifuged at full power (16100 rcf), 20 ºC for 15 minutes, and the supernatant (cell lysate) was separated from the cell pellet carefully using a 20-200 µL pipette.

Freeze-thaw cycles

After 5 freeze/thaw cycles (2 hours at -80 ºC/1 hour thawing at room temperature), the cells were centrifuged and the supernatant was collected in the same way that was used in the ultra-sonication approach.

The collected cell lysate was diluted with 100 µL of the mobile phase, aliquoted to 2 x 10^6 cells per sample (50 µL) and frozen (-80 °C) before being subjected to subsequent sample preparation steps.

The same procedure was used for Golgi fractions, except for some adjustments that are illustrated in **Figure 13**.

2.6.2 Sample clean-up

Amicon Ultra centrifugal filter (10 K) were pre-rinsed (as recommended by the producer) with 400 µL type 1 water to remove glycerine, which is found in trace amounts in the filter membrane and may interfere with the analysis, and centrifuged at full power (16100 rcf), 20 ºC for 10 minutes. 50 µL of standard, cell lysates or Golgi fractions samples were applied to the filters and centrifuged at 16100 rcf, 20 ºC for 10 minutes, and then 50 µL of washing solution (ACN/100 mM ammonium carbonate, 95/5, v/v) was added and centrifuged again at the same conditions to elute the retained analyte.

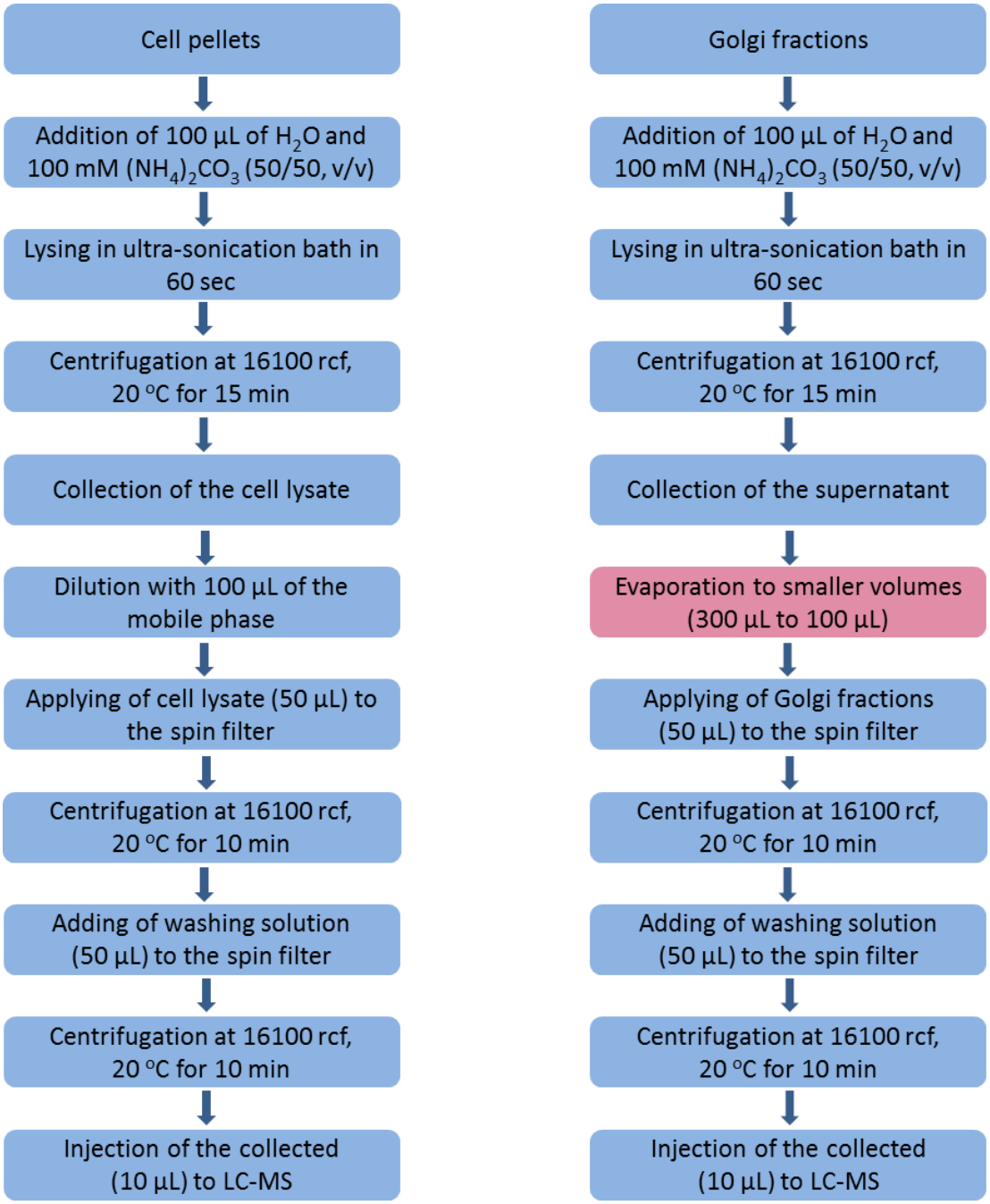

Figure 13: Schematic view of lysing and sample preparation for the cell pellets and Golgi fractions.

2.7 LC-MS system

2.7.1 Mobile phases

Mobile phases were prepared by mixing ACN, 100 mM ammonium carbonate and type 1 water in different ratios. Mobile phase with 50, 55, 60, 65, 70 and 75 % ACN,

with an ionic strength of 20, 25 or 30 mM were prepared during the optimization of the method (**Table 3**).

Table 3: Overview of mobile phases with various ionic strengths and organic content.

ACN %	**50 %**	**55 %**	**60 %**	**65 %**	**70 %**	**75 %**
Molarity in the MP	ACN/type 1 H_2O/100 mM $(NH_4)_2CO_3$, v/v/v					
20 mM	50/20/30	55/20/25	60/20/20	65/20/15	70/20/10	75/20/5
25 mM	50/25/25	55/25/20	60/25/15	65/25/10	70/25/5	75/25/0
30 mM	50/30/20	55/30/15	60/30/10	65/30/5	70/30/0	75/25*/0

* Ammonium carbonate concentration was 120 mM.

2.7.2 Columns

ZIC-*p*HILIC columns (2.1 x 150 mm, 5 µm) used in the development and application of the method were from Sequant (Umeå, Sweden) [80]. Polyether ether ketone (PEEK) tubings with 0.10, 0.13 and 0.18 mm ID) were from Upchurch Scientific (Oak Harbour, WA, USA).

2.7.3 Preliminary study LC-MS instrumentations

Preliminary experiments were performed using a Waters 2695 Separations Module and a Micromass ZQ single quadrupole equipped with an ESI source from Waters (Milford, MA, USA). The pump flow was set to 200 µL/min and the injection volume was 10 µL. ESI source was used in negative mode with a capillary voltage set to 2.5 kV, a cone voltage 30 V, a source temperature and desolvation temperature of 150 and 140 °C, respectively. Drying gas and nebulizer gas were applied at 250 and 50 L/hr, respectively. Data were collected with SIM mode (*m/z* 426.0 and 505.9) using MassLynx software version 4.1 from Waters.

For MS/MS analysis, an Ultimate 3000 UHPLC system coupled to a TSQ Vantage triple quadrupole MS (Thermo Scientific) equipped with an ESI source was used. The flow rate of the mobile phase was set to 200 µL/min and the injection volume was 10 µL. The analyte was ionized using ESI in negative mode with a spray voltage of 2500 V, a capillary temperature of 350 °C, a sheath gas pressure of 35 psi and collision energy of 40 V. Xcalibur Software (Thermo Scientific) was used for controlling the MS

and for data collection. SRM mode with the transition *m/z* 426.0 → *m/z* 79.0, 134.0, 158.9, 328.0 was used.

A 2695 Separations Module from Waters and a TSQ Quantiva™ triple quadrupole MS (Thermo Scientific, Waltham, MS, US) were also used for MS/MS analysis with the same MS parameters as used with the Vantage MS.

2.7.4 Main study LC-MS instrumentations

LC analyses were performed using an Alliance® Waters 2695 Separation Module and a Micromass Quattro *micro* API Mass Spectrometer with ESI from Waters. The flow rate was 200 µL/min and the injection volume was 5 µL. Ionization was performed in negative mode with a capillary voltage of 3 kV, cone voltage of 45.0 V and extractor voltage of 3 V. Source temperature and desolvation temperature were 100 and 150 °C, respectively. Drying gas and nebulizer gas were applied at 250 and 10 L/hr, respectively. The chromatograms were obtained from MassLynx software version 4.1 (Waters), and PAPS was monitored in SIM mode *m/z* 426.0 and 505.9.

2.8 Regeneration of the column

Column regeneration was performed by rinsing the column with strong salt solution at low flow rate in the reverse direction. The rinsing procedure was to wash the column with 30 column volumes (3 mL) of type 1 water, 30 column volumes of 0.5 M sodium chloride and 30 column volumes of type 1 water at a flow rate of 100 µL/min.

2.9 UV measurements (NanoDrop™)

To prepare the samples, 50 µL of cell lysate samples were applied to the spin filters which were centrifuged at 16100 rcf for 10 minutes at room temperature. The filters were then washed with 50 µL of solutions containing 10, 50, 65, 90, 95, 100 % ACN and 90, 50, 35, 10, 5 % 100 mM $(NH_4)_2CO_3$ (v/v) sequentially, and centrifuged (16100 rcf, 10 minutes, room temperature). To compare/assess protein content of prepared samples, 2 µL of sample was subjected to UV spectroscopy using the NanoDrop™ unit (measured at 280 nm).

2.10 Gel electrophoresis

This section was performed together with Tore Vehus (PhD student at bioanalytical chemistry, Department of Chemistry, UiO). The six collected solutions from section **2.9** were evaporated to dryness and re-dissolved in 50 µL Tris-HCl. 10 µL of 1X SDS sample loading-buffer (1% (w/v) SDS, 1 mM DTT, 20% (v/v) glycerol, 20 mM Tris–HCl pH 7.0 and 0.01% (w/v) bromophenol blue) were added to the samples, which were heated at 70 °C for 15 min to denature the proteins, and subsequently cooled at room temperature for a few minutes. 15 µL of the samples and PageRuler™ Prestained Protein Ladder were loaded onto NuPAGE®Novex®12% Bis–Tris protein gels and separated for 30 minutes at 150 V in 1X MOPS running buffer. After separation, the gel was washed with water type 1 and kept in methanol/acetic acid/water (50/10/40, v/v/v) for 24 hours. The gel was then washed with water, soaked in Coomassie Blue Staining solution (10% (v/v) acetic acid, 0.005% (w/v) Coomassie Brilliant Blue and 90% (v/v) water) for two hours and subsequently de-stained in (methanol/acetic acid/water, 50/10/40, v/v/v) for 24 hours.

2.11 Calculations

The recovery (R %) was obtained by comparing the peak area of PAPS in the samples spiked before ultrafiltration (a), with the peak area of PAPS in the samples spiked after ultrafiltration (b).

$$R\ \% = \frac{a}{b} * 100$$

Precision of the method is expressed as the relative standard deviation RSD (%).

$$RSD\ (\%) = \frac{SD}{mean} * 100$$

SD is the standard deviation of the values.

3 Results and discussion

Based on our experience with separation of nucleoside triphosphates [65], a ZIC-*p*HILIC column was chosen as stationary phase for the quantitative determination of PAPS. However columns with small particles and small inner diameter provide high efficiency and sensitivity, ZIC-*p*HILIC columns with small particles and ID were not available. The parameters influencing the retention and efficiency of PAPS in *p*HILIC e.g. organic modifier content and ionic strength are presented. A simple and effective sample preparation is also presented, before robustness issues with ZIC-*p*HILIC and PAPS stability are examined. At the end, the method is evaluated.

3.1 MS detection

The first step in LC-ESI-MS method development was to find the optimal MS parameters for detection of PAPS. A standard solution of PAPS (100 µg/mL) was infused directly to the MS with negative ESI. Two *m/z* were observed in negative ESI-MS mode (**Figure 14**).

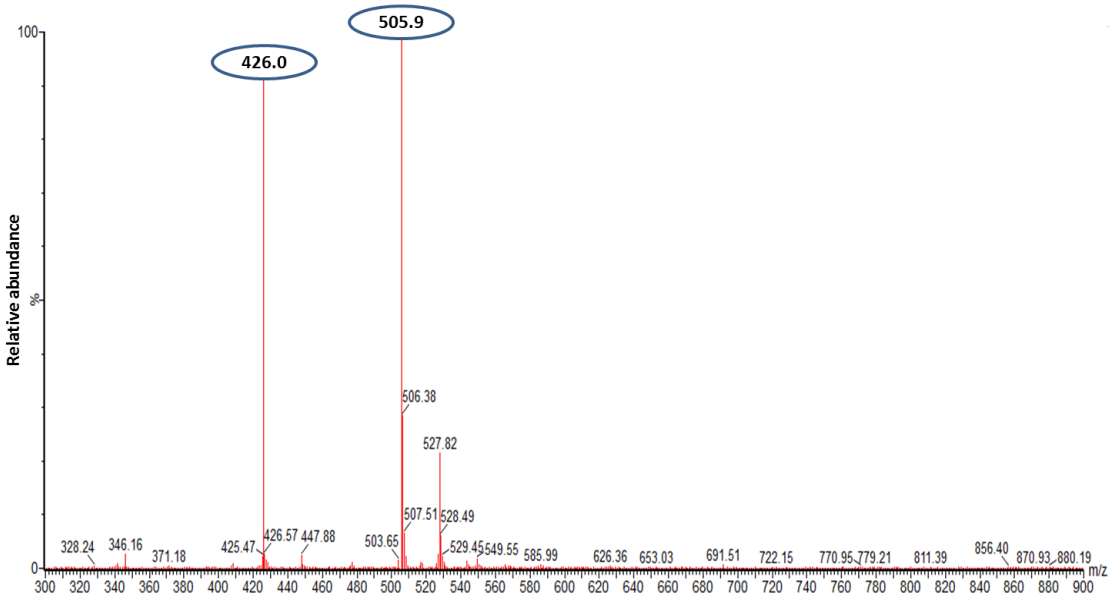

Figure 14: ESI-MS of 100 µg/mL standard solution of PAPS. Direct injection, negative mode, and full scan data acquisition in range of *m/z* 300 – 900.

It was observed that the sulfate group is cleaved off from PAPS molecules in ESI source to produce *m/z* 426.0 in addition to *m/z* 505.9 (**Figure 15**).

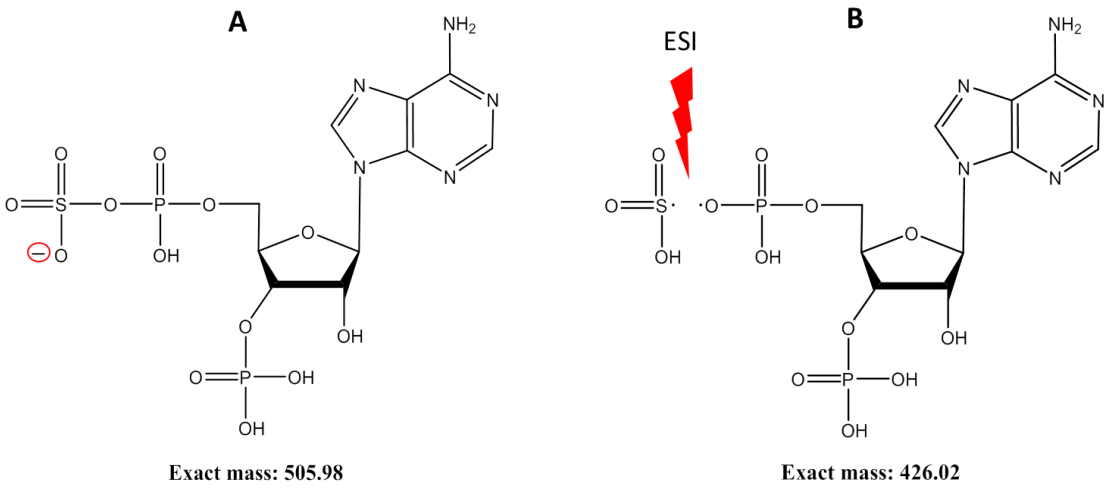

Figure 15: PAPS in ESI. **A)** Shows the predictable ionization of PAPS that may occur in the MP by missing a proton (H^+) to produce *m/z* 505.9 in the ESI. **B)** Shows the sulfate group which is cleaved off from PAPS in the ESI to produce *m/z* 426.0.

The analyte was not necessarily easy to detect, and much time was spent on the optimization of the MS parameters. For instance, the TSQ Vantage triple quadrupole MS did not give any particular response even after a month of optimization attempts.

3.2 Optimizing ZIC-*p*HILIC efficiency

3.2.1 Organic content of the mobile phase

A method with a relatively short analysis time (defined here as less than 10 minutes) and with satisfactory chromatographic efficiency and repeatability was sought. It is known that in HILIC mode, increasing the content of ACN in the MP will typically leads to a reduction of the elution strength, which will increase the retention time [14, 51].

Several mobile phases (50, 55, 60, 65, 70 and 75 % ACN) were tested to obtain an acceptable retention time. The aqueous part of the mobile phases was water and a volatile buffer of ammonium carbonate (100 mM, described in section **3.2.2**). The PAPS standard solutions were dissolved in the used mobile phase in each analysis. In HILIC, it is recommended that the composition of the sample solvent should be as close as possible to the initial mobile phase to avoid peak distortion and poor efficiency, which are related to the difference in the viscosity and polarity between the MP and the sample solvent [81-83]. The mobile phases with 50, 55, 60 and 65 %

ACN offered relatively stable retention times, below 10 minutes, shown in **Figure 16.** On the other hand, when 70 % ACN in the mobile phase was used, for unknown reasons, the retention time was very unstable (varied from 4.9 up to 10.8 min), as shown in **Figure 41** in appendix. A mobile phase with 75 % ACN displayed a longer retention time (13 minutes) surpassing the desired analysis time limit of 10 minutes.

The MP with 65 % ACN gave the highest repeatability in peak area (RSD (%) = 3, n = 3) and the highest efficiency of N = 2870 (N per m = 19100), compared to 1500 (N per m = 10000), 1470 (N per m = 9800) and 2150 (N per m = 14300) for mobile phases containing 60, 55 and 50 % ACN, respectively. The efficiencies were satisfactory compared to the efficiency of *p*HILIC columns (N per m = 12927 and 14159) for related compounds [65].

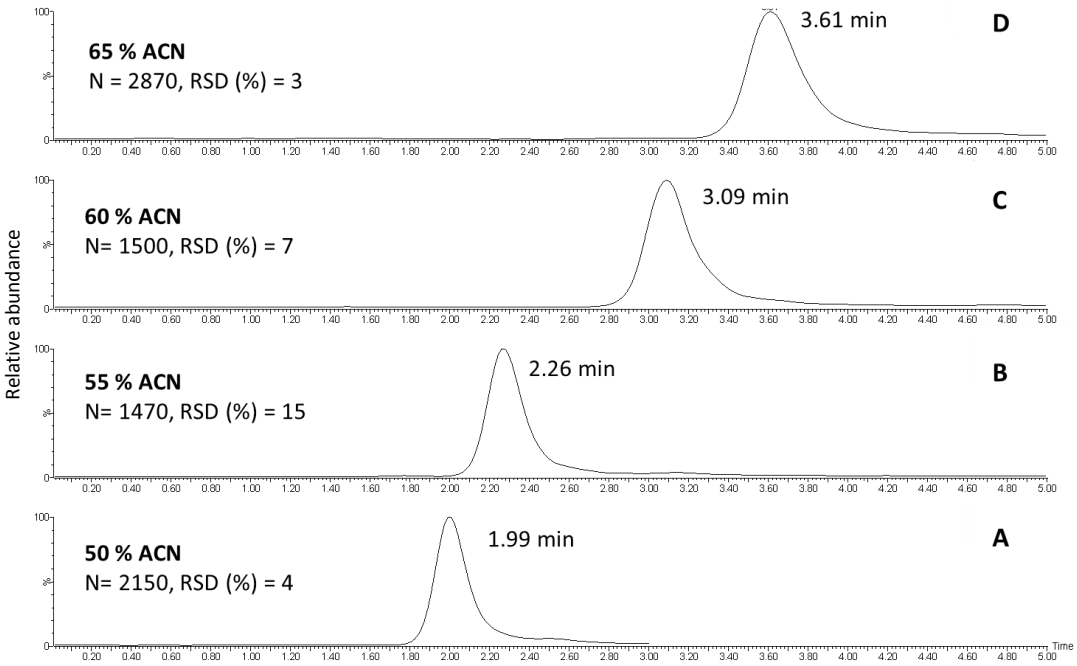

Figure 16: The retention time of PAPS as a function of ACN content. Chromatograms of 100 µg/mL PAPS standard solutions dissolved in the MP using a ZIC-*p*HILIC column (2.1 × 150 mm, 5 µm) with mobile phases consisting of A) 50, B) 55, C) 60 and D) 65 % ACN and 30 mM ionic strength in the aqueous part of the MP (see **Table 3**) at flow rate of 200 µL/min. The injection volume was 10 µL. MS detection (ESI, single quadruple), negative ionization mode, SIR (*m/z* 426.0 and 505.9) was used.[4]

[4] In later stages of the study, changes in the retention time of PAPS occurred due to aging of the column, as seen in **Figure 30, 32, 35, 36** and **38**. Since *p*HILIC columns are expensive, the aging (but functional) column was used throughout the study.

The mobile phase with 65 % ACN gave reasonable retention time, lowest RSD (%) of peak area and highest efficiency, and was used in subsequent studies.

3.2.2 Ionic strength of the mobile phase

The ionic strength of the mobile phase has to be selected carefully since it has a considerable impact on the retention (due to ionic interactions between the analyte and the stationary phase), efficiency and MS signal [84]. Ammonium salts are often used in HILIC due to their solubility in mobile phases with high organic content and their volatility when mass spectrometry is used [24, 62, 64]. Even though a moderate pH of the mobile phase could ensure ionization of PAPS (pK_a is 1.59 [85]), a relatively high pH (~ 8) was used as it was preferred for separation of similar analytes like ATP and ADP [65]. Ammonium carbonate was considered as an appropriate option due to its volatility, solubility and high pH buffering capacity (pK_a = 9.2) [65].

Table 4 shows the effect of increasing ionic strength (20 → 30 mM) of the mobile phase on the efficiency and the retention time. The efficiency, represented by the plate number, was improved with increasing ionic strength. Mobile phases of 30 mM total ionic strength offered best efficiencies. No significant difference in the retention times was observed.

Table 4: The retention time and efficiency of PAPS as a function of the ionic strength in mobile phase on a ZIC-*p*HILIC column. Other chromatographic conditions were as described in **Figure 16**.

	Retention time (min)			
$(NH_4)_2CO_3$	50 % ACN	55 % ACN	60 % ACN	65 % ACN
20 mM	1.9	2.3	3.1	3.8
25 mM	1.9	2.2	3.1	3.8
30 mM	1.9	2.2	3.0	3.6
	Efficiency (N)			
20 mM	1480	1000	1840	1070
25 mM	1640	1040	1410	1110
30 mM	2150	1470	1500	2870

The salt concentration in the MP can have a significant impact on the sensitivity of ESI-MS [86]. As seen in **Figure 17**, the MS signal (represented by the peak area) was adversely affected by salt concentrations due to the ion suppression, which may take place when high salt concentration are used [35]. Although the lower ionic strength mobile phases produced the higher sensitivity, the efficiency (N) was considered more important in the study.

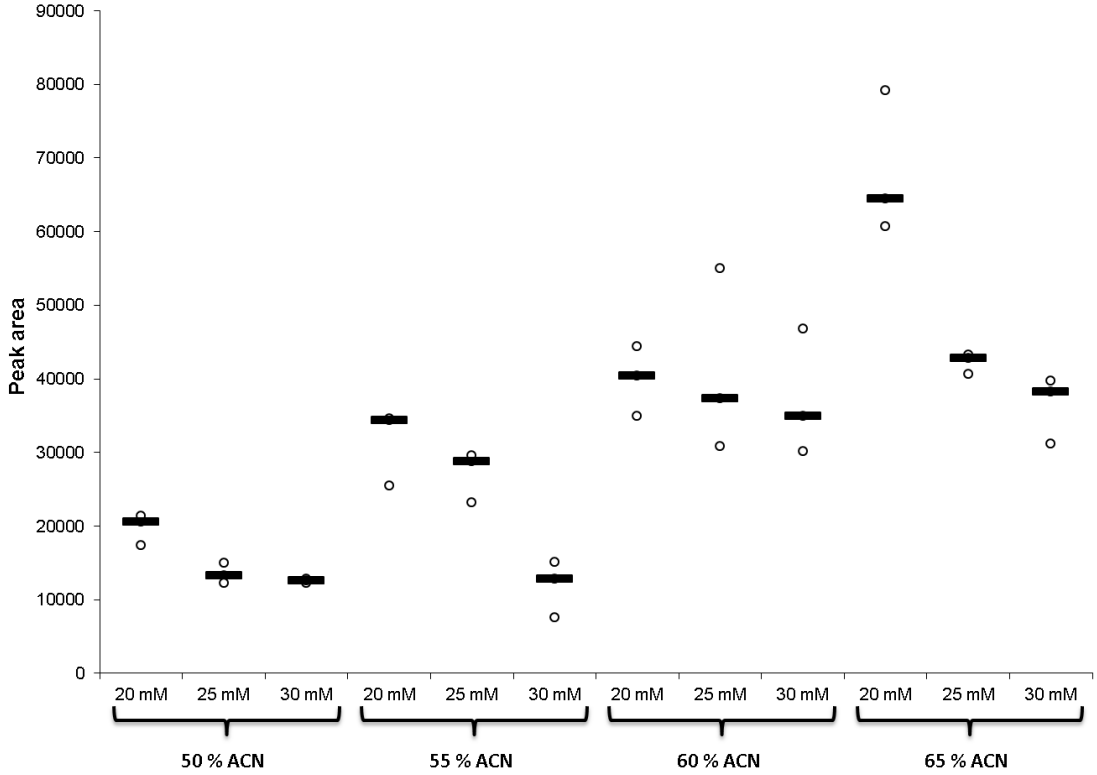

Figure 17: Peak area of PAPS (represent the sensitivity of MS) as a function of ACN % and salt concentration in the MP. 100 µg/mL standard solutions of PAPS (n = 3) were injected when 50, 55, 60 and 65 % ACN used in MP. Other chromatographic conditions were as described in **Figure 16**.

The mobile phase with 65 % ACN and 30 mM ammonium carbonate was adapted as the MP for the method, as it gave reasonable retention time and sensitivity and the highest efficiency.

3.3 Sample preparation development

3.3.1 Preliminary studies on standard solutions

Centrifugal ultrafiltration was selected for isolating the analyte from potentially interfering proteins in the cell samples, because it is a rapid, simple and effective sample preparation method [67, 73]. In initial experiments, aqueous standard solutions were directly applied to the spin filters, without any pretreatment, and centrifuged. The achieved recovery of PAPS was very poor. For enhancing the recovery, a subsequent washing step was performed after applying the standard solution in order to release analytes adsorbed to the filter's membrane (**Figure 18**).

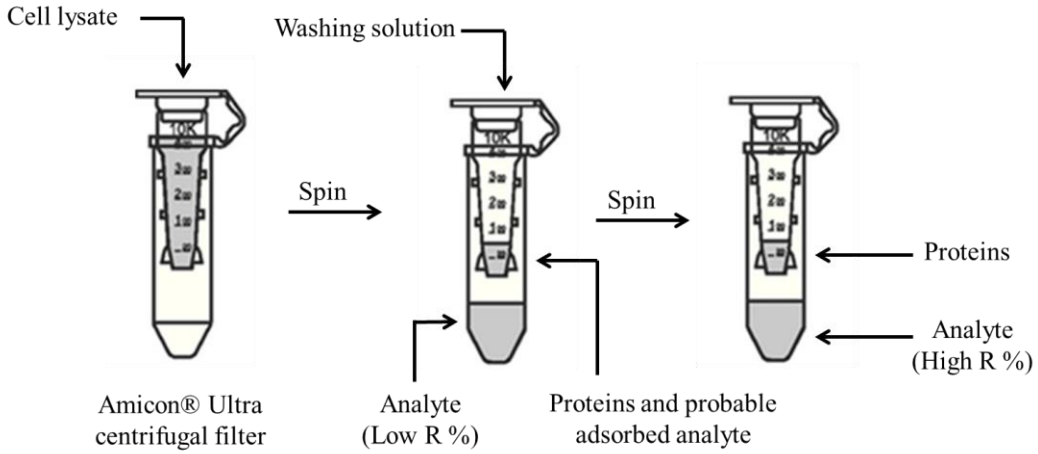

Figure 18: Sample clean-up procedure. The sample was applied to spin filter, centrifuged, washed and centrifuged. The figures of the Ultra centrifugal filter were reproduced from [74].

To assess the optimum washing conditions in terms of recovery, different amounts of organic solvent in the washing step were tested (**Figure 19**). At first, a solution of ACN, 100 mM $(NH_4)_2CO_3$ and type 1 water (65/30/5, v/v/v) was used as a washing solution (A chromatogram), as it was the composition of the MP. The applied standard solution contained 35 % ACN, 65 % H_2O (100 mM $(NH_4)_2CO_3$ and type 1 water), so the final solution from filtration contained 50 % ACN and 50 % H_2O. This approach produced a recovery of less than 75%, and PAPS peak had a substantial tailing and was divided into two peaks (**Figure 19 A**). The peak splitting was likely related to the large amount of water (50 %) in the filtered samples compared to the MP, that may decrease the partitioning of the analyte into the water-layer on the stationary phase and lead to poorer efficiency and lower retention

[62, 87]. To improve the recovery and peak shape, the total water amount in the washing solution, and consequently in the injected samples, was decreased by washing the filter with solutions of ACN/100 mM of $(NH_4)_2CO_3$ (90/10, 95/5 and 100/0, v/v) (**Figure 19 B**, **C** & **D**), resulting in final water concentration of 37.5, 35 and 32.5 %, respectively. Chromatogram B shows higher recovery (84 %), but the splitting of the peak increased. Chromatogram C shows even higher recovery (89 %) and a peak without splitting. This improvement in the peak shape is a result of that the final solution contains exactly the same water amount as the MP (35 %). Reducing the water content even more by washing with 100 % ACN as in the D chromatogram, increased the recovery up to more than 90 %. However, a larger degree of peak tailing was observed, likely because the water amount in the final solution (32.5 %) was less than that in the MP.

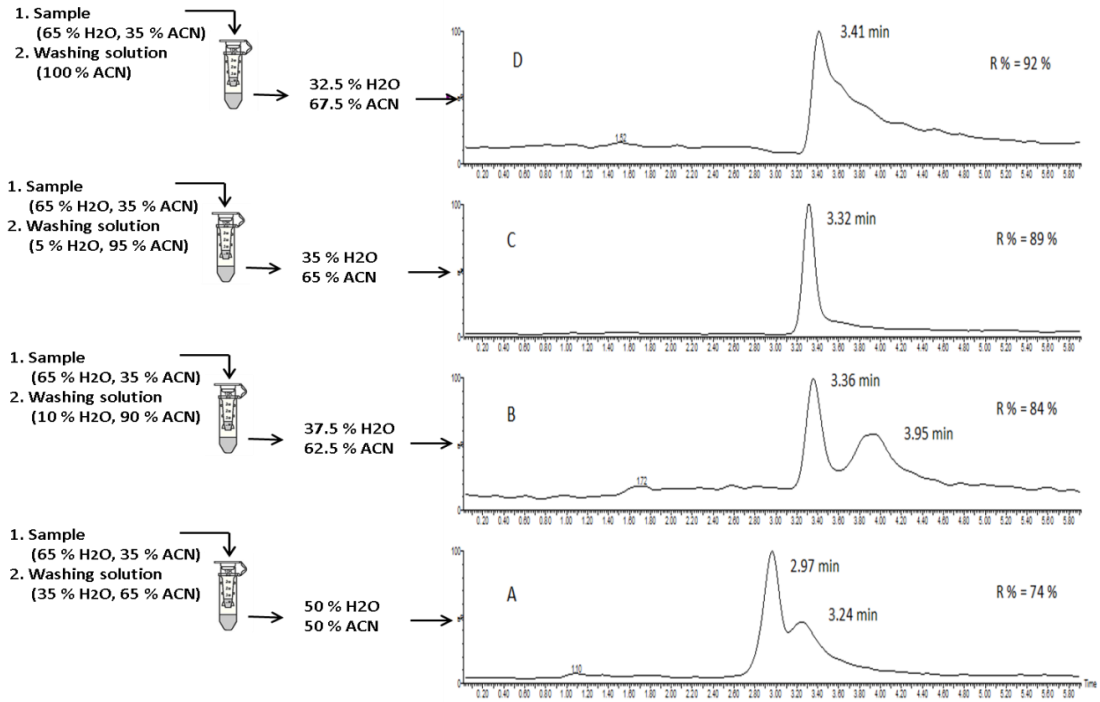

Figure 19: Chromatograms of PAPS (right) as a function of water content in the filtrated samples prepared as shown to the left in the figure. Chromatograms of 50 µg/ml standard solutions of PAPS were applied to the spin filters and washed with different washing solutions A) 65 % ACN and 35 % $(NH_4)_2CO_3$ (100 mM), B) 90 % ACN and 10 % $(NH_4)_2CO_3$ (100 mM), C) 95 % ACN and 5 % $(NH_4)_2CO_3$ (100 mM) and D) 100 % ACN. H_2O in the figure refers to the aqueous part (water and $(NH_4)_2CO_3$ (100 mM)) and R % is recovery %. The chromatographic conditions were as described in **Figure 16**.

*Thus, ACN/100 mM $(NH_4)_2CO_3$ (95/5, v/v) was chosen as the washing solution for the main studies since it produced acceptable recovery and efficiency (**Figure 19 C**).*

3.3.2 Biological samples

The same sample preparation procedure used for standard solutions was tested for biological samples to examine the recovery. Three MDCK I cell lysate samples were centrifuged and spiked with PAPS to concentration levels of 25, 37.5 and 50 µg/mL after ultrafiltration. Three other MDCK I cell lysate samples were spiked with an appropriate amount of standard solution to give concentrations of 50, 75 and 100 µg/mL (to correct for the 2 X dilution after the washing step) before ultrafiltration.

The recovery was determined to be 62-75 % (not corrected for with an internal standard) and was considered to be acceptable (**Figure 20**).

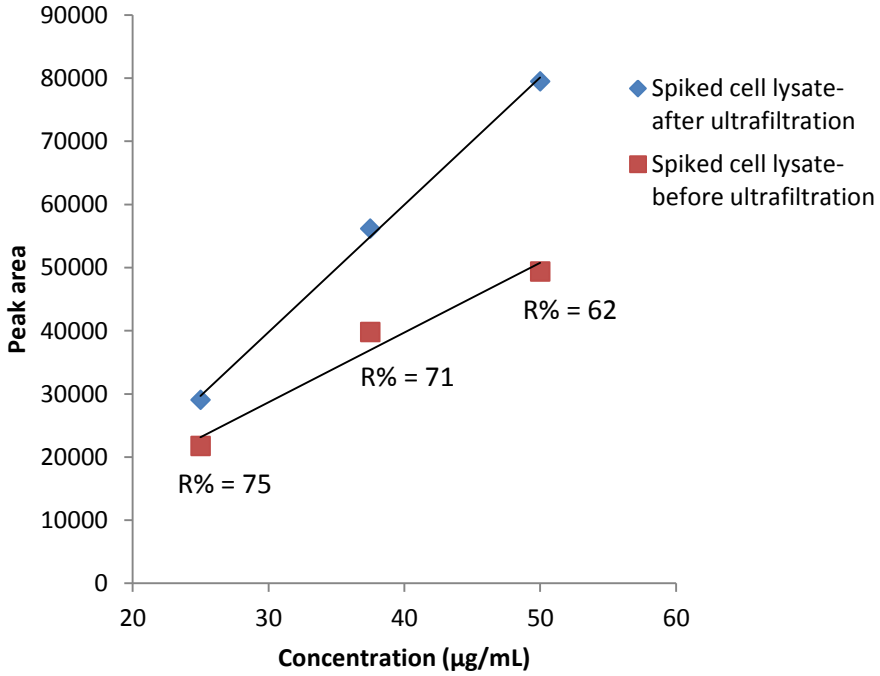

Figure 20: Recovery (R %) of PAPS in real samples. Cell lysate samples spiked with PAPS before and after filtration to 25, 37.5 and 50 µg/mL were used to find recovery. The chromatographic conditions were as described in **Figure 16**.

3.4 Robustness issues with *p*HILIC

3.4.1 Retention time shift

During the application of the method for cell lysates, an increase in retention time (**Figure 21**) and back pressure was observed. Two different volumes (5 and 10 µL) of the cells lysates were injected to study the impact of injection volume (**Figure 21**). The retention time increased approximately 0.1 min for each ten injections. A potential reason for the changing retention time is binding of retained undesired debris to the stationary phase [62]. At the same time, the increased back pressure (from 90 to 110 bar during 100 injections) could occur due to the precipitation of some matrix components (proteins, lipids etc.) that might clog the inlet frit and lead to increasing pressure [62].

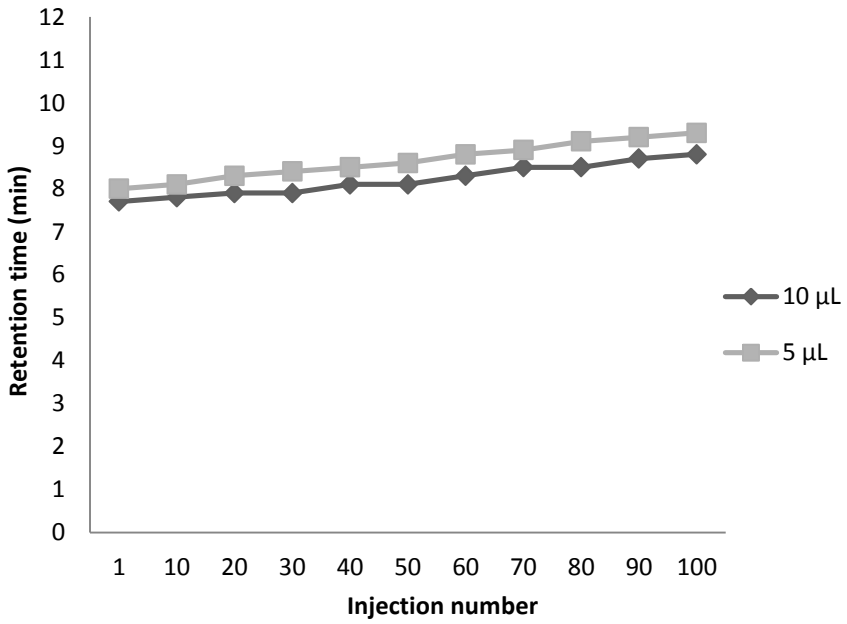

Figure 21: Retention time of PAPS for 100 injections of the cell lysate samples. 5 and 10 µL were used as injection volumes. The chromatographic conditions were as described in **Figure 16**.

Figure 22 illustrates the behaviour of the retention time after 100 injections of Golgi fractions. Golgi fractions show the same trend in the retention time shifting as cell lysates.

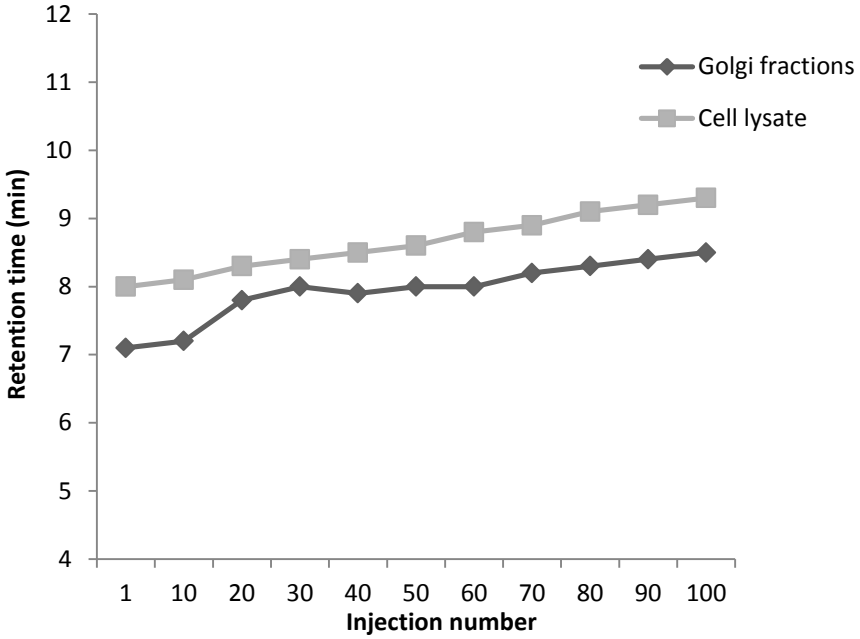

Figure 22: Retention time of PAPS for 100 injections of the cell lysate samples and Golgi fractions. Injection volume was 5 µL. The chromatographic conditions were as described in **Figure 16**.

3.4.2 Proteins

Although the recovery was acceptable for biological samples, variation/increasing in the retention time and the backpressure of the column were observed when analysing cell samples. It was speculated that the variation was due to the presence of proteins in the ultrafiltrated cell lysate samples after the washing step with a high content organic solution (ACN/100 mM $(NH_4)_2CO_3$, 95/5, v/v). The protein amount in the ultrafiltrated samples was assessed using NanoDrop™ UV spectroscopy (**Figure 23 A**) and gel electrophoresis (SDS-PAGE) (**Figure 23 B**). Washing solutions with different ACN amounts (ACN/100 mM $(NH_4)_2CO_3$, 10/90, 50/50, 65/35, 90/10, 95/5, 100/0, v/v) were used to reveal possible effect of ACN quantity on the spin filter's ability to discard proteins. However, no noticeable differences in protein presence in the ultrafiltrated samples could be observed (**Figure 23**).

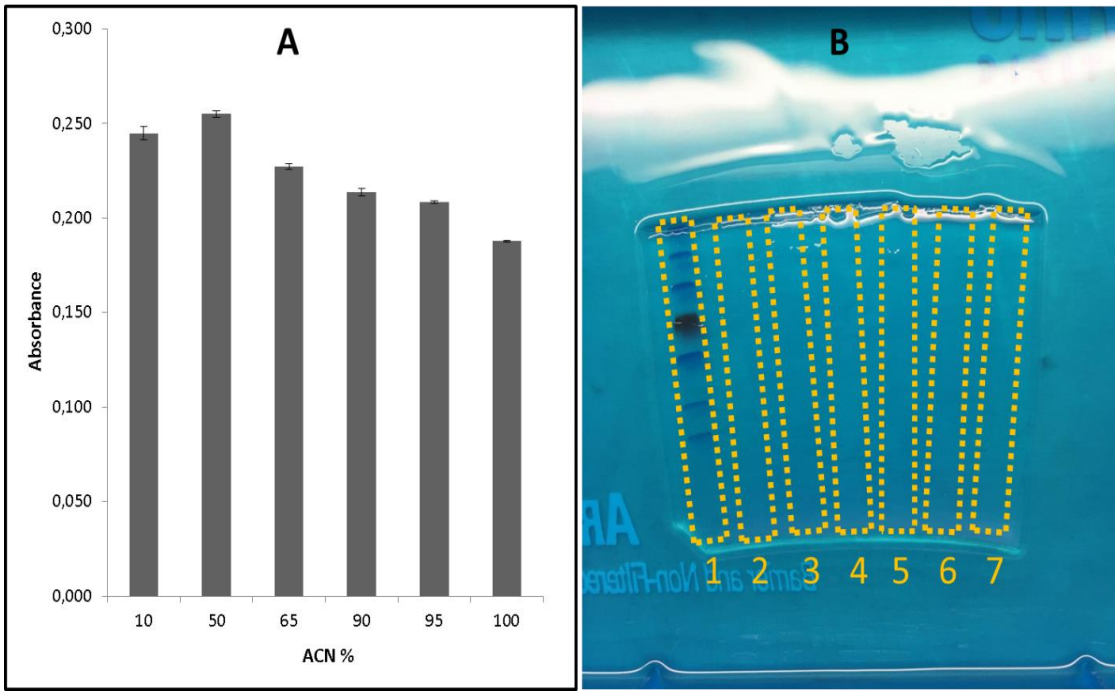

Figure 23: Proteins assessment. **A)** Absorbance (280 nm) of 2 µL of the ultrafiltrated cell lysates after the washing step with various ACN amounts (n = 3). **B)** Picture of SDS-PAGE. The protein ladder[5] and the ultrafiltrated samples (ACN/100 mM $(NH_4)_2CO_3$, 10/90, 50/50, 65/35, 90/10, 95/5, 100/0, v/v) were applied in the 1, 2, 3, 4, 5, 6 and 7 lanes of the gel, respectively. The yellow dotted lanes on **B** were added by the author of the thesis.

The ultrafiltrated samples that were obtained after washing the filters with ACN and 100 mM $(NH_4)_2CO_3$ (10/90, 50/50, 65/35, 90/10, 95/5, 100/0, v/v), were prepared to gel electrophoresis as described in section **2.10** before applying in lanes 2-7 of the gel (**Figure 23 B)**, respectively. No protein is seen in lanes 2-7 compared to protein ladder. That means the ultrafiltrated samples are free of proteins, and proteins are not responsible for the increasing in the retention time.

3.4.3 Effect of washing

To avoid the continuous increase of the retention time, the column was rinsed whenever the retention time had increased about 10 % (after 60-70 injections). Since the normal procedure to regenerate the column is considered as a time and effort consuming and non-automatable process (described in section **2.8**), a more uncomplicated and effortless process was tested. The column was washed with a mixture containing ACN, ammonium carbonate (100 mM) and type 1 water (50/30/20, v/v/v) at flow rate of 200 µL/min for 30 minutes without reversing the

[5] Protein ladder is a set of standard proteins used to estimate the size of a molecule in gel electrophoresis.

flow direction in the column. After the washing, the retention time was measured and compared to the retention time of the normal washing procedure as shown in **Figure 24**. Both washing procedures, normal and simple, could bring the retention time back to the original values.

Thus, the simple washing procedure was adopted as a rinsing procedure in the further work because it was rapid, did not require reversing the flow direction in the column, and gave satisfactory regeneration.

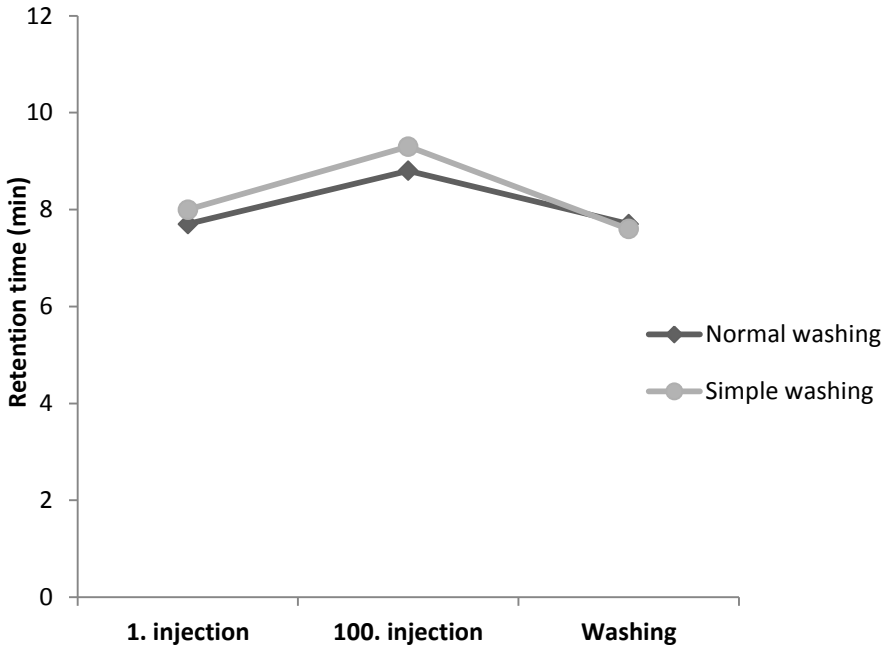

Figure 24: Retention time of PAPS on the *p*HILIC column using the normal and the simple washing procedures after 100 injections of cell lysates and Golgi fractions. The chromatographic conditions were as described in **Figure 16**.

3.4.4 Golgi samples

Golgi fractions from the various cell lines were provided in large volumes (2-3 mL), and were evaporated using Speed-Vac® for enrichment. The enriched solution had a very dense texture, similar to a syrup **(Figure 25, right)**, due to presence of sucrose in Golgi fractions. Sucrose was added during the isolation of Golgi fraction using a sucrose gradient procedure **(Figure 25)**. To remove sucrose and avoid formation of this dense solution that cannot be injected in LC-MS system, the isolated Golgi fraction was diluted 3 times with 1X PBS and subjected to centrifugation at 50000 rpm for 1 hour at 4 ºC. The supernatant was discarded and the pellets were

diluted with 1X PBS and again centrifuged. Finally, 200 µL of PBS was added to the pellets. Isolation of Golgi fractions and removing of sucrose are described in detail in section **6.2.3** in appendix.

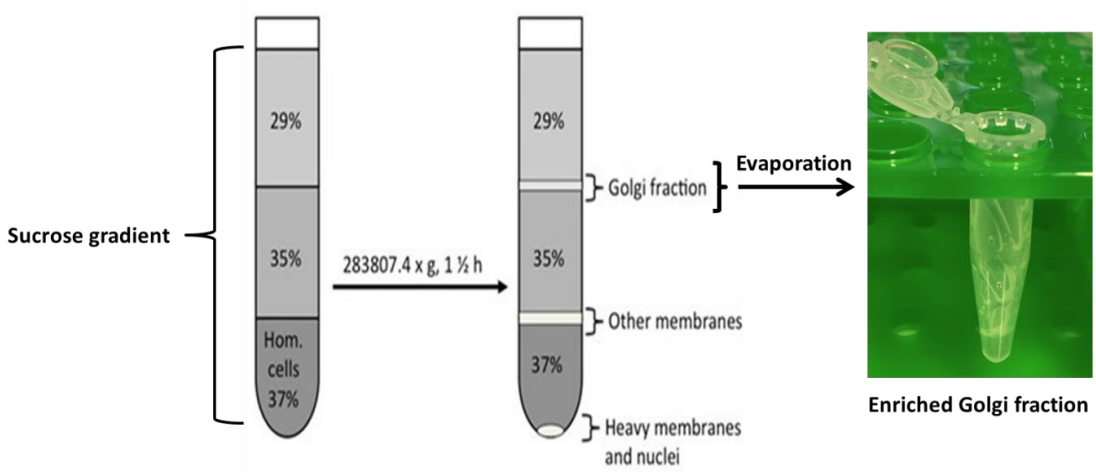

Figure 25: Isolation and enrichment of Golgi fractions. **Left)** Sucrose gradient was used for isolation of Golgi fractions. **Right)** 1 mL of isolated Golgi fraction evaporated for 2 hours. The figure of sucrose gradient was reproduced from [88].

3.5 PAPS stability

After optimizing the chromatographic conditions including organic content and ionic strength in the MP, as well as the sample preparation process, the stability of PAPS under various conditions was investigated as it is a prerequisite for reliable quantitative determination [89].

3.5.1 Stability of standard solutions

With the aim of defining the potential storing conditions for the samples (in the auto-sampler etc.) when the method is introduced to routine analyses, and evaluating the stability of PAPS under freezing and thawing (used for cell lysing), 3 replicates of 10 µg/mL standard solutions of PAPS were prepared and each replicate was divided into six aliquots. The first three aliquots were analysed immediately after preparation. Three others were used to check the stability of PAPS after 24 hours storage at room temperature (18 ºC), in the fridge (4 ºC) and in the freezer (-80 ºC), and two were used to test the stability after five and ten freeze-thaw cycles. As seen in **Figure 26**, after 24 hours storing PAPS was more stable in the samples stored at room

temperature compared to those in the fridge and the freezer. Furthermore, ten freeze-thaw cycles of the standard solutions showed much lower intensity than only five cycles. As a consequence, the samples were preferably stored at room temperature and freezing/thawing was not used as a cell disruption method in the further applications and method evaluation.

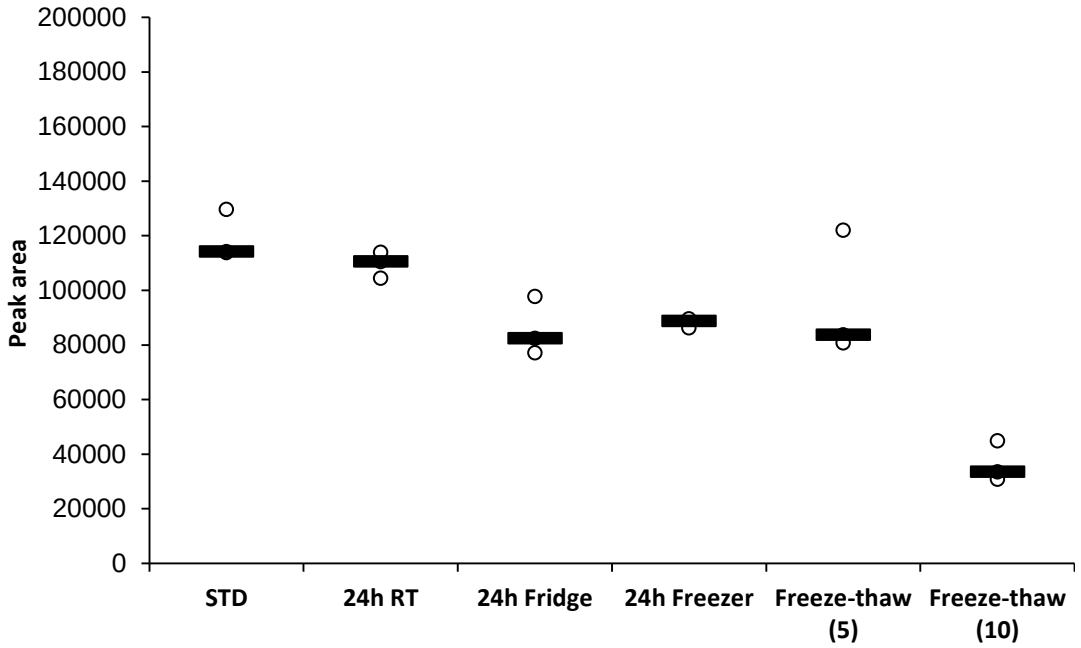

Figure 26: Peak area of PAPS standard solutions as a function of the storage conditions. Three replicates at each condition were analysed using the same conditions as described in **Figure 16**.

3.5.2 Cell lysate samples

To test stability of PAPS in the stored cell lysates (as opposed to cell pellets), MDCK II and MDCK B22 cell pellets were lysed by ultra-sonication as described in section **2.6.1**. The cell lysates were stored at -80 ºC up to five days; the sample preparation steps were done on the day of the analysis. As seen in **Figure 27** the cell lysates were stable at least five days at -80 ºC. Increasing in the MS signal can be in charge of the significant increasing in the peak areas in the all cell lysates on the fourth day since they are not corrected for with an internal standard.

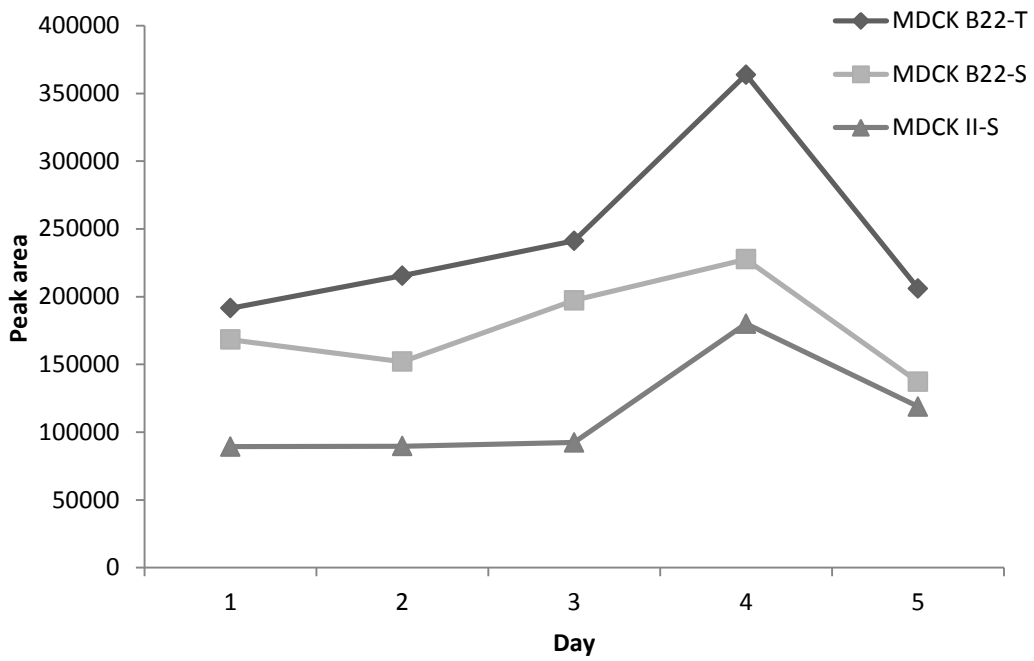

Figure 27: Peak area of PAPS in cell lysate samples stored at -80 ºC. Cell lysates of MDCK II and MDCK B22 (trypsinized (T) and scraped (S)) were stored at -80 ºC and analysed over five days. Sample preparation was performed daily. Injection volume was 5 µL. The chromatographic conditions were as described in **Figure 16**.

To test the influence of sample preparation process on the cell lysates stability, MDCK I and MDCK B22 prepared cell lysates were stored at room temperature for 24 hours and analysed after 0, 5, 1, 2, 3, 4 and 24 hours. The peak area of PAPS was quite similar after 24 hours storing at room temperature (**Figure 28**). Therefore, the prepared samples can be stored at room temperature (in the auto-sampler etc. when the method is introduced to routine analyses) for at least 24 hours without any significant degradation.

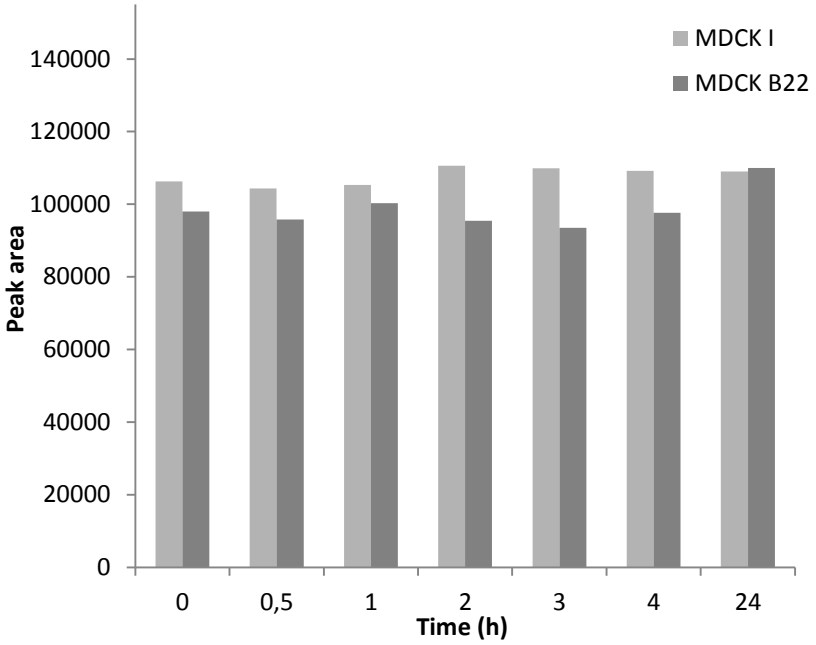

Figure 28: Peak area of PAPS in prepared cell lysate samples for 24 hours at room temperature. Cell lysates of MDCK I and MDCK B22 were stored at room temperature for 24 hours after sample preparation. Injection volume was 5 µL. Other chromatographic conditions were as described in **Figure 16**.

3.5.3 Stability of PAPS under evaporation

With the purpose of enriching Golgi fractions by evaporation using Speed-Vac®, the stability of PAPS during evaporation in Speed-Vac® was examined. 1 mL of a 100 ng/mL standard solution was evaporated to ~ 100 µL to obtain a concentration of 1 µg/mL. 10 µL of the enriched standard solution was injected on the column as well as a standard solution with a concentration of 1 µg/mL. The signal intensity of the enriched standard solutions was approximately equal to that of the standard solution, with recovery of 105 % (**Figure 29**).

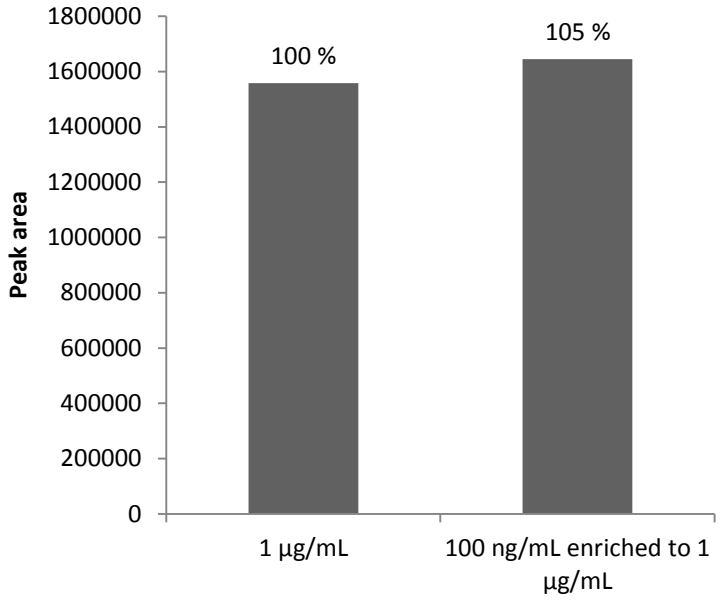

Figure 29: Peak area of PAPS under evaporation. A standard solution of 1 µg/mL and a standard solution of 100 ng/mL enriched to 1 µg/mL in the Speed-Vac® were analysed using Quantiva™ MS instrument in SRM mode (*m/z* 426.0 → *m/z* 79.0, 134.0, 158.9, 328.0). Other chromatographic conditions were as described in **Figure 16**.

3.6 Preliminary investigation of PAPS in samples

The developed method was applied for analysis of different cell line samples. A representative chromatogram of MDCK B22 cell line analysis is shown in **Figure 30**. As seen in chromatogram (b) in **Figure 30**, the sample contains two more compounds in addition to PAPS with the same MS profile. These two compounds were identified as being ADP and ATP (using external standards). The molar mass of ATP is 507.0, which is similar to that for PAPS (506.99), therefore it has same *m/z* (505.9) after ionization (deprotonation) in the mobile phase/ESI as PAPS. In addition, a phosphate group is cleaved off from ATP molecules in-source to produce *m/z* 426.0 (**Figure 31**) (like PAPS in **Figure 15**). ADP is ionized (deprotonated) in the MP/ESI, and produces an *m/z* of 426.0 in the ESI (**Figure 31).** Since ATP and ADP have exactly the same *m/z* as PAPS, they could be seen in the SIM chromatograms with PAPS. This will not be a problem for determination of PAPS in cells as ADP and ATP are separated (in the column) from PAPS, due to the selectivity of the *p*HILIC approach.

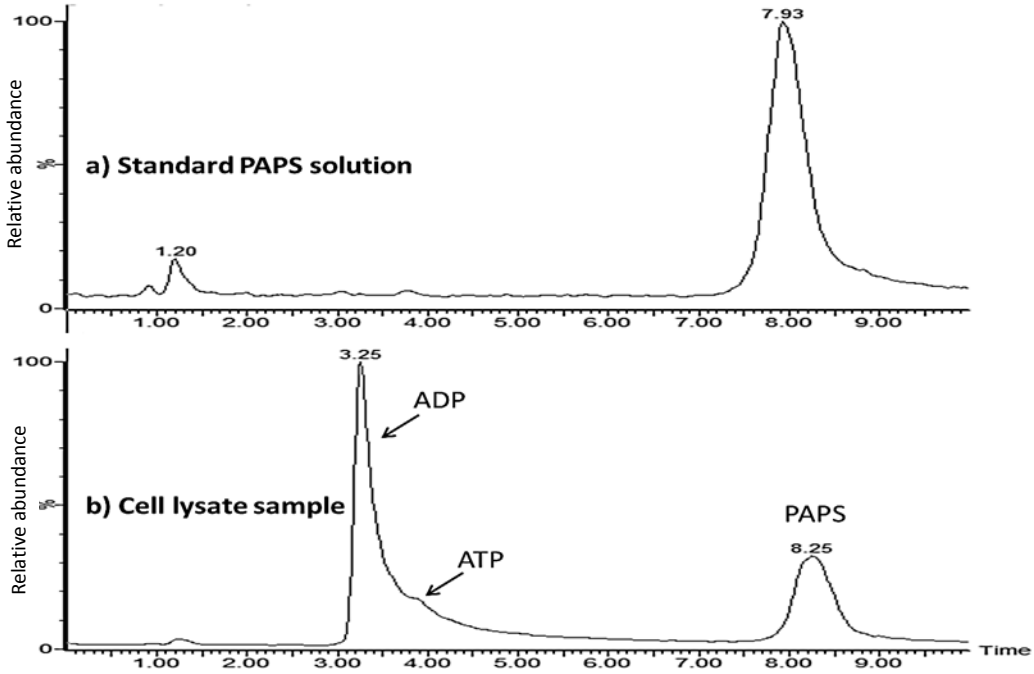

Figure 30: SIM (*m/z* 426.0, 505.9) chromatogram of standard PAPS solution and cell lysate samples. **a)** SIM (*m/z* 426.0 and 505.9) of a 10 µg/mL standard solution and **b)** SIM (*m/z* 426.0 and 505.9) of MDCK B22 cell lysate (2×10^6 cells per sample). Chromatographic conditions were as described in **Figure 16**.[6]

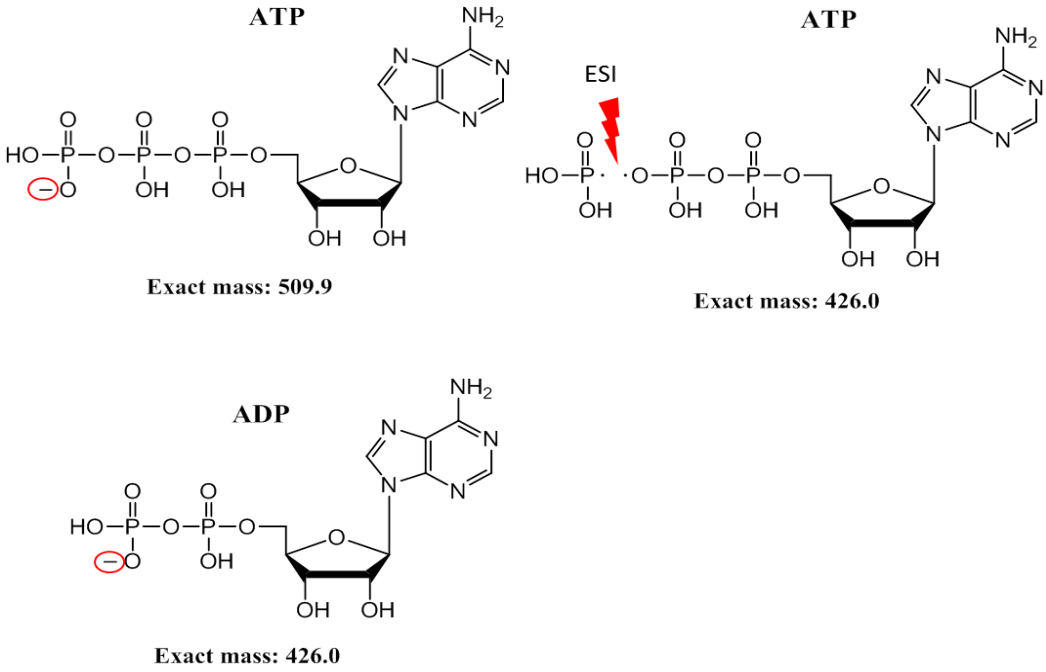

Figure 31: ATP and ADP in ESI. **Left**) The predictable ionization of ATP and ADP that may occur in the MP by missing a proton (H^+) to produce *m/z* 505.9 and 426.0, respectively. **Right**) A phosphate group is cleaved off from ATP in the ESI to produce *m/z* 426.0.

[6] A change in the retention time of PAPS can be seen in **Figure 30** and the next figures. The efficiency of the column with the new retention times was found to be (N = 2379), which is quite similar to the efficiency with the original retention time (N = 2867).

In addition, the method was also applied for Golgi fractions analysis. **Figure 32** shows a chromatogram of the upper Golgi fraction (UG) of MDCK B22 cells.

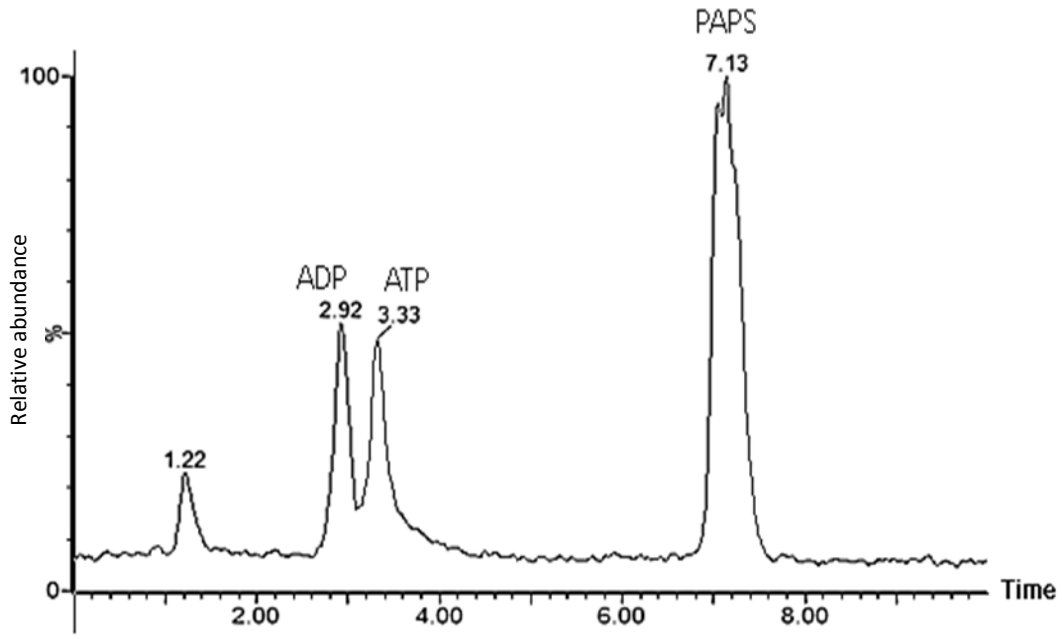

Figure 32: SIM (*m/z* 426.0, 505.9) chromatograms of Golgi fraction samples. SIM (*m/z* 426.0 and 505.9) of upper Golgi fraction of MDCK B22. Chromatographic conditions were as described in **Figure 16**.

Gradual reduction of PAPS levels was observed in the presence of the competitive PAPS synthesis inhibitor chlorate [90]. **Figure 33** and **Figure 34** show this reduction of PAPS levels in cells and Golgi fractions when they were treated with various concentrations of sodium chlorate[7]. The small rise of the peak area for PAPS (**Figure 34**) in the presence of 0.5 and 1 mM chlorate is expected, as a stimulation of sulfation of certain molecules (heparan sulfate) at low chlorate concentrations has been observed [91]. The probable explanation of this phenomenon is that the PAPS transporter in the Golgi membrane is able to reduce the K_m value (increase affinity) so that it takes in more PAPS into the Golgi lumen, while less will remain in the cytoplasm. From **Figure 34,** the concentration of PAPS in cells was estimated to be 3 µg/mL (0.14 nmol/10^6 cells), which is low compared with the concentrations stated in the other methods (0.4 – 0.8 nmol/10^6 cells). One explanation may be that reduced selectivity of previous methods has led to an overestimation of levels.

[7] Chlorate is an *in vitro* inhibitor of ATP-sulfurylase, which is the first enzyme in the biosynthesis of PAPS (Figure 4). Chlorate replaces sulfate in the active site of the enzyme, thus sulfation mechanisms are affected [90].

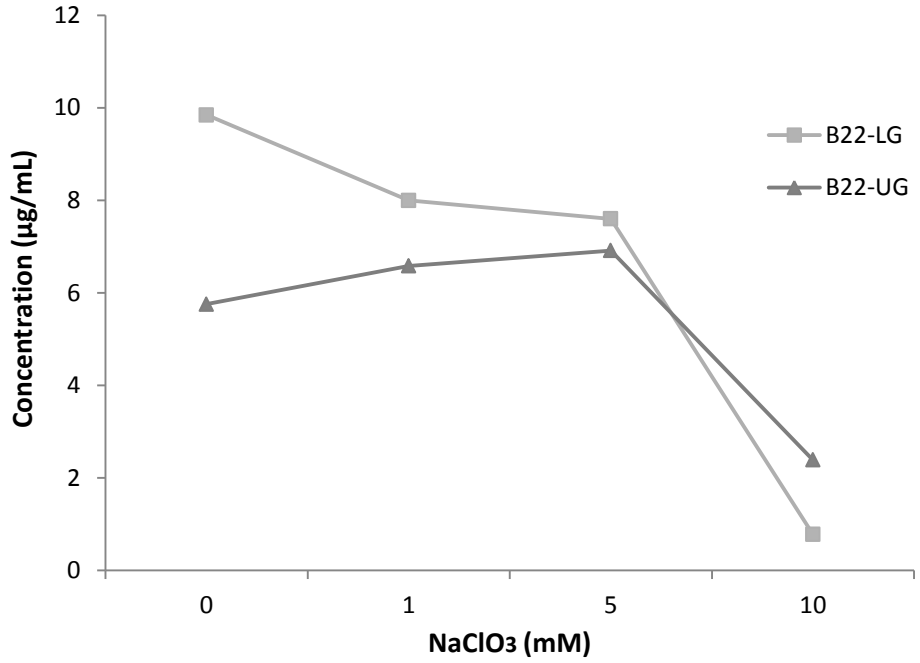

Figure 33: Concentration of PAPS (µg/mL) in Golgi fractions as a function of sodium chlorate concentration. Golgi fractions (Upper (UG) and lower (LG) fraction) of MDCK B22 treated with 0, 1, 5 and 10 mM of sodium chlorate. The chromatographic conditions were as described in **Figure 16**.[8]

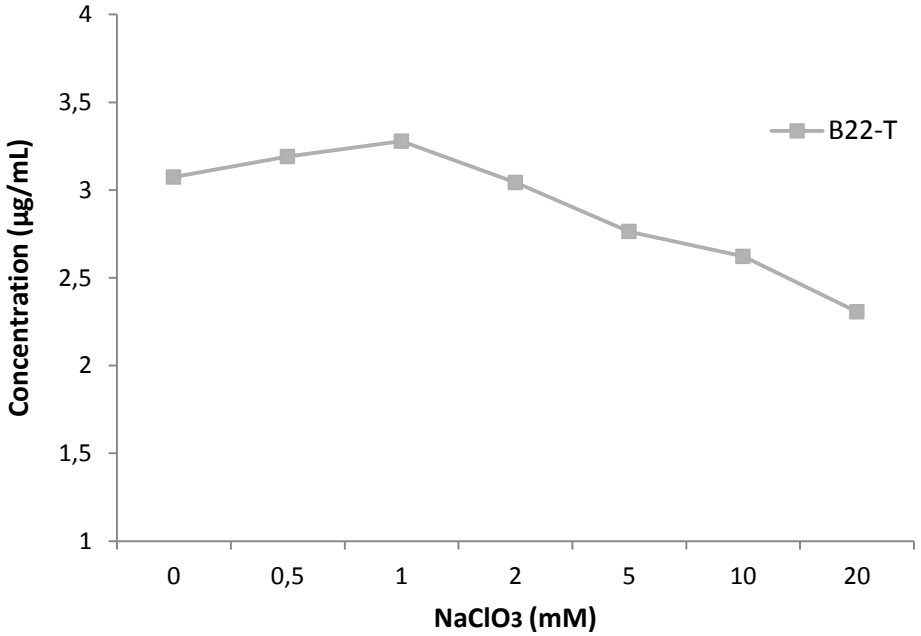

Figure 34: Peak area of PAPS in cells as a function of sodium chlorate. MDCK B22 (trypsinized) cell pellets treated with 0, 0.5, 1, 2, 5, 10 and 20 mM of sodium chlorate. The chromatographic conditions were as described in **Figure 16**.

The method shows results that are consistent with the biologically expected.

[8] The concentrations in **Figure 33** and **Figure 34** were estimated by a single point calibration curve.

3.7 Method evaluation

To be obtain a status of high reliability, a method has to be extensively validated by evaluating a range of parameters, including linearity, limit of detection, limit of quantification and repeatability of measurement [19]. In this thesis, a complete validation (long term study, e.g. several operators, instruments and time points) has not been carried out due to time limitations. However, an evaluation of the key parameters is presented in the following.

3.7.1 Internal standard

To correct for any analyte loss during sample preparation and variance of the ionization efficiency in MS, an internal standard (IS) was employed during the method evaluation. The internal standard must behave like the analyte during sample preparation and analysis, and must not be naturally present in the sample [19]. With MS detection, it was possible to use an isotope labeled PAPS (^{13}C-PAPS) as an internal standard (**Figure 35**).

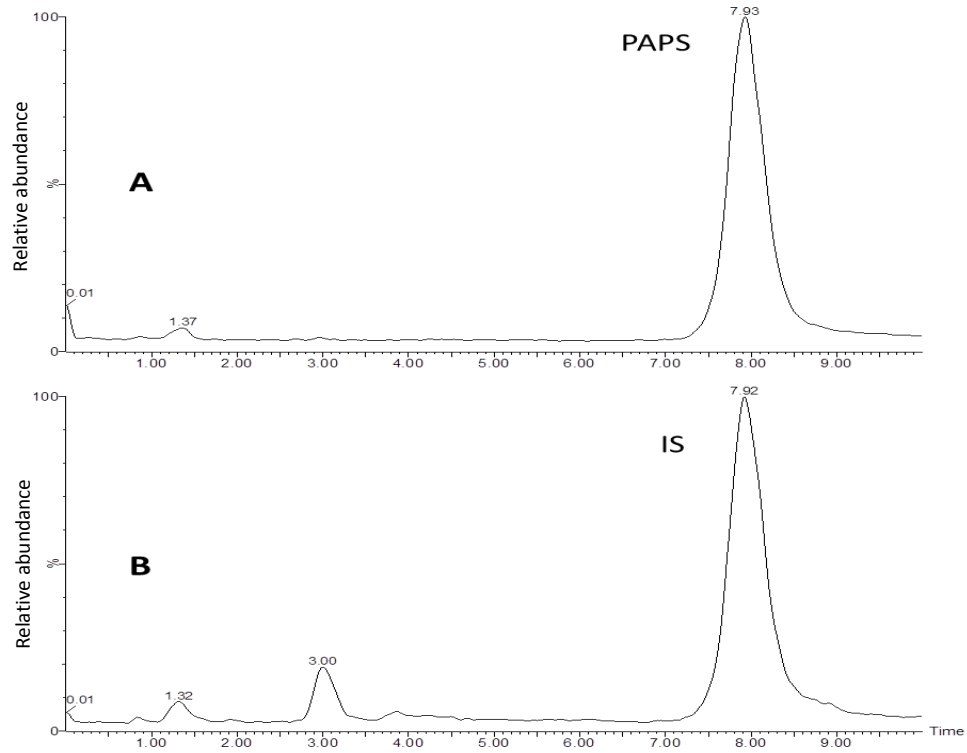

Figure 35: Internal standard. Chromatograms of a standard solution contain PAPS and IS in a concentration of 10 µg/mL for both. **A**) SIM *m/z* 426.0, 505.9 shows PAPS and **B**) SIM *m/z* 436.0, 516.0 shows IS. Chromatographic conditions were as described in **Figure 16**.

3.7.2 Limit of detection and limit of quantification

As analyte-free biological samples are seemingly not available and since the recovery of the analyte was satisfactory, standard solutions were used to determine the detection/quantification limits. The concentration limit of detection (cLOD) is the lowest concentration of an analyte that can be detected, and can provide a signal to noise ratio S/N of 3 or greater [19]. A concentration of 0.5 µg/mL (2.5 ng injected on the column in 5 µL) was found to be the cLOD in the method (**Figure 36**), and this corresponds to 2 ng/10^5 cells (assuming 100 % recovery). For concentrations lower than 0.5 µg/mL only noise was observed.

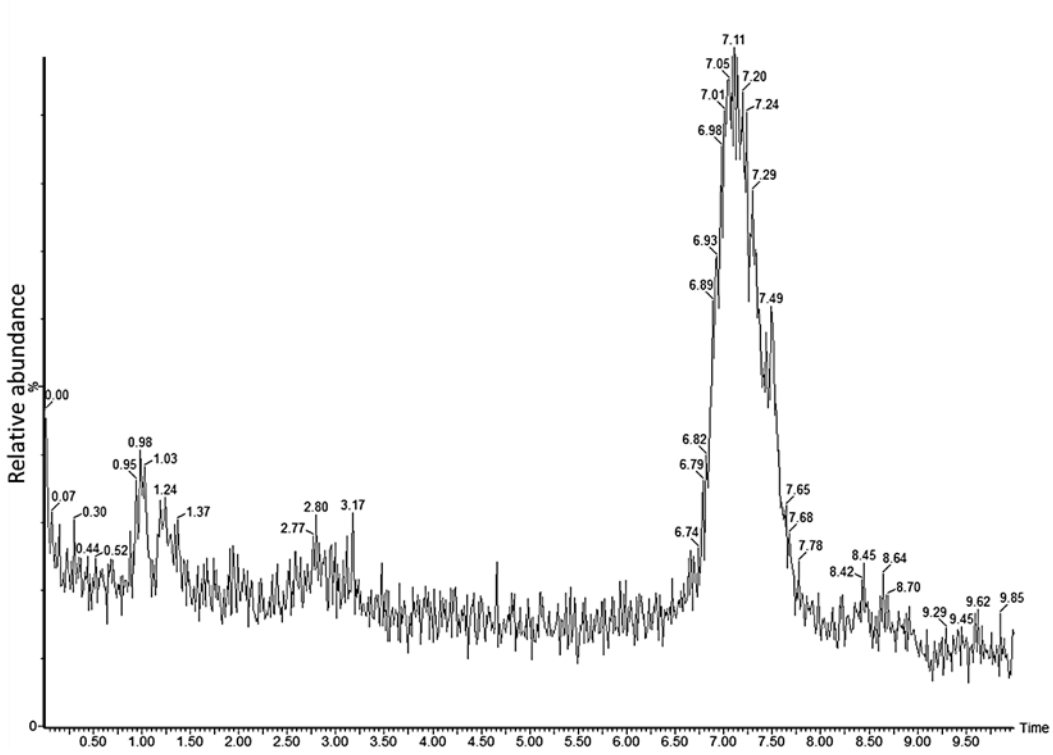

Figure 36: SIM chromatogram of 0.5 µg/mL PAPS standard solution. Injection volume was 5 µL. Other chromatographic conditions were as described in **Figure 16**.

The concentration limit of quantification (cLOQ) is the lowest concentration of an analyte that can be quantified with suitable precision and accuracy (RSD % ≤ 20), and can provide a signal to noise ratio S/N of 10 [19]. The cLOQ in the method was found to be 2 µg/mL (10 ng injected on the column in 5 µL), and this corresponds to 8 ng/10^5 cells (assuming 100 % recovery) with an RSD (%) of 13. The cLOQ is quite high, however, it was suitable for analysis of the samples in this project. The cLOQ of the method can be improved by employing a newer and thus more sensitive mass spectrometers or tandem MS.

3.7.3 Linearity

The linearity of the method was investigated in the range from 2 to 200 µg/mL. Six replicates contain PAPS at four concentration levels 2, 10, 100 and 200 µg/mL and IS at a concentration of 10 µg/mL were prepared in spiked cell lysate samples (1 x 10^5 cells per sample), and were used to obtain the data. The peak area ratio of PAPS over IS against the ratio of their concentrations as plotted in **Figure 37**. The linearity was assessed by determining the square linear regression for the line of best fit. As illustrated in **Figure 37**, the method has a good linearity for the entire concentration range ($R^2 > 0.99$).

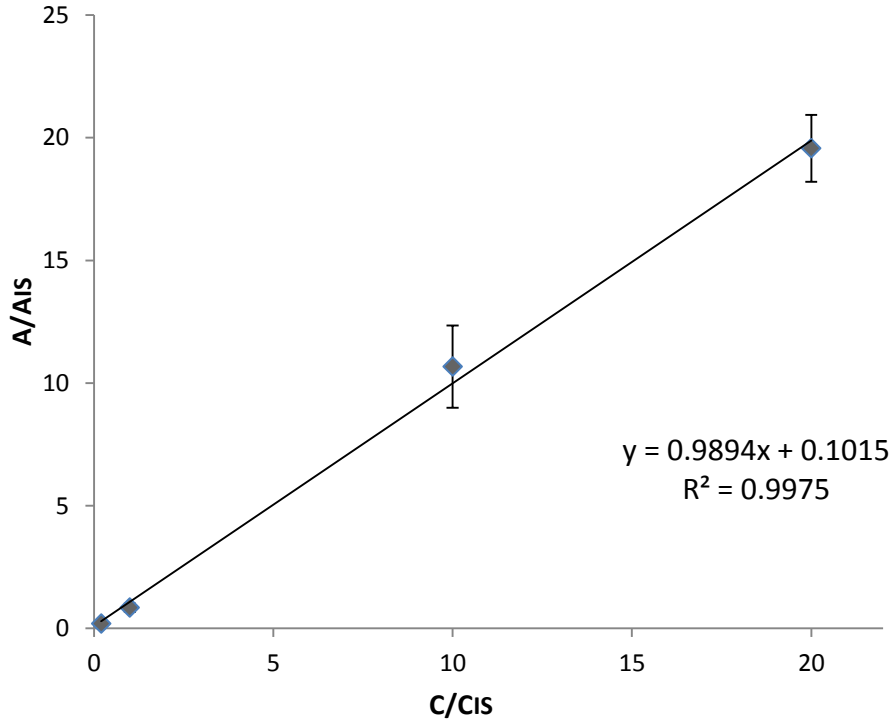

Figure 37: Peak area of PAPS/peak area of IS (A/A_{IS}) as a function of their concentration ratio (C/C_{IS}) in the range from 2-200 µg/mL PAPS and 10 µg/mL IS. Data were obtained by single injection of six replicates at each concentration level. Injection volume was 5 µL. Chromatographic conditions were as described in **Figure 16**.

3.7.4 Precision

The precision of the method was established at four concentration levels (2, 10, 100 and 200 µg/mL), and expressed as the relative standard deviation RSD (%). Within-day repeatability of the method was examined by spiking 6 cell lysate samples

at each concentration level before ultrafiltration. The samples were prepared and analysed on the same day. **Table 5** shows the results.

Table 5: Intra-day precision of A/A_{IS} for PAPS concentration 2-200 µg/mL and IS concentration of 10 µg/mL. Chromatographic conditions were as described in **Figure 16**.

Concentration (µg/mL)	n	RSD (%)
2	6	16
10	6	19
100	6	16
200	6	6.9

Between-day repeatability was also examined by the spiked cell lysates. Three new replicates at each concentration level were prepared and analysed over five days. The results are shown in **Table 6**.

Table 6: Inter-day precision of A/A_{IS} for PAPS concentration 2-200 µg/mL and IS concentration of 10 µg/mL. Chromatographic conditions were as described in **Figure 16**.

Concentration µg/mL	n	RSD (%)
2	5	20
10	5	15
100	5	3.7
200	5	4.1

Within- and between-day precisions were found satisfying for the method. The RSD (%) values were lower than 20 %, except for the between-day precision at the lowest concentration level. Calculations are shown in section **6.6.1** in appendix.

3.7.5 Selectivity

Selectivity of a method is the ability of the method to distinguish between an analyte and other potential interferences in the sample such as other analytes and matrix components. The method was found to be selective since it has the ability to separate PAPS from other interfering analytes that have the same precursor ion mass and product ion mass as PAPS (e.g. ATP); see previous figures **Figure 30** and **Figure 31.**

3.7.6 Carry-over

Carry-over is a system contamination from the previous sample which causes analyte peaks to re-appear in the following blank injection. The accuracy and the precision of the method can be affected if the system contains carry-over [92]. Carry-over was investigated by performing a blank injection of mobile phase after samples during the validation of the method, as well as throughout the study. As seen in **Figure 38** no carry-over was observed.

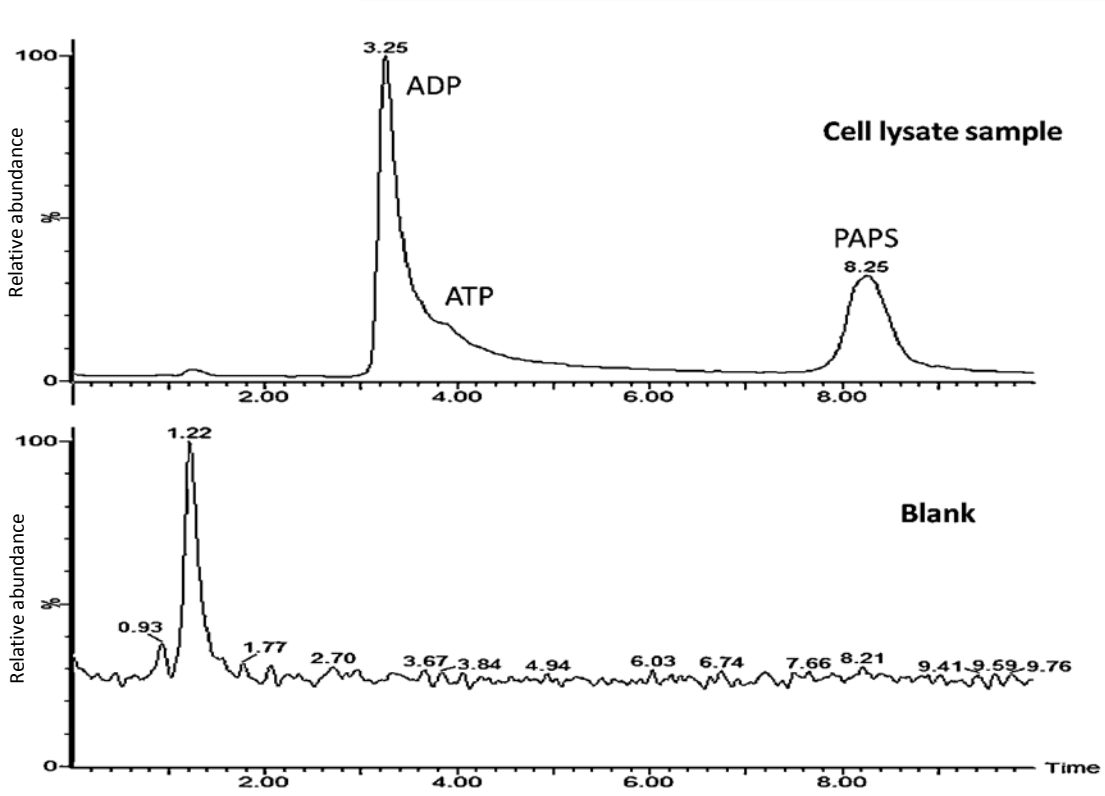

Figure 38: Upper: SIM (*m/z* 426.0, 505.9) chromatogram of a cell lysate sample. Lower: SIM (*m/z* 426.0, 505.9) chromatogram of a blank injection (5 µL of the mobile phase). Other chromatographic conditions were as described in **Figure 16**.

The method was evaluated, and it e.g. has a good linearity (R^2 > 0.99), satisfactory within- and between-day repeatability (RSD (%) < 20) and acceptable cLOD (0.5 µg/mL) and cLOQ (2 µg/mL).

4 Conclusion

As hypothesized in the aim of study, ultra centrifugal filtration for simple and rapid sample preparation followed by *Z*IC-*p*HILIC-ESI-Quadrupole-MS for selective detection were indeed suited for determining PAPS in different MDCK cell lines and their Golgi fractions. In support of the method's validity, a reduction in PAPS levels in cells and Golgi fractions was observed when treated with chlorate (a PAPS synthesis inhibitor) as it was biologically expected.

In the future, the focus may be put on further refining of the sample preparation to increase the number of injections before a regeneration of the column is needed. A comprehensive validation of the method (with internal standard) can also be carried out for securing very reliable quantitation of PAPS in cells and Golgi fractions. A newer MS or tandem MS could be employed in order to acquire more sensitive and selective detection, when necessary.

5 References

[1] K.K. Murray, The term "multiple reaction monitoring" is recommended, Rapid Communications in Mass Spectrometry, 29 (2015) 1926-1928.

[2] Z.-H. Xu, T.C. Wood, A.A. Adjei, R.M. Weinshilboum, Human 3′ -Phosphoadenosine 5′ -Phosphosulfate Synthetase: Radiochemical Enzymatic Assay, Biochemical Properties, and Hepatic Variation, Drug Metabolism and Disposition, 29 (2001) 172-178.

[3] M.W.H. Coughtrie, S. Sharp, K. Maxwell, N.P. Innes, Biology and function of the reversible sulfation pathway catalysed by human sulfotransferases and sulfatases, Chemico-Biological Interactions, 109 (1998) 3-27.

[4] G. Dick, L.K. Akslen-Hoel, F. Grøndahl, I. Kjos, M. Maccarana, K. Prydz, PAPST1 regulates sulfation of heparan sulfate proteoglycans in epithelial MDCK II cells, Glycobiology, (2014).

[5] yourgenome.org, What is a cell?. http://www.yourgenome.org/facts/what-is-a-cell, accessed 24.05.2016.

[6] T. Wang, I. Cook, T.S. Leyh, 3′ -Phosphoadenosine 5′ -Phosphosulfate Allosterically Regulates Sulfotransferase Turnover, Biochemistry, 53 (2014) 6893-6900.

[7] C.D. Klaassen, J.W. Boles, Sulfation and sulfotransferases 5: the importance of 3'-phosphoadenosine 5'-phosphosulfate (PAPS) in the regulation of sulfation, The FASEB Journal, 11 (1997) 404-418.

[8] S. Besset, J.B. Vincourt, F. Amalric, J.P. Girard, Nuclear localization of PAPS synthetase 1: a sulfate activation pathway in the nucleus of eukaryotic cells, The FASEB Journal, 14 (2000) 345-354.

[9] K.V. Venkatachalam, Human 3'-phosphoadenosine 5'-phosphosulfate (PAPS) Synthase: Biochemistry, Molecular Biology and Genetic Deficiency, IUBMB Life, 55 (2003) 1-11.

[10] G. Dick, F. Grøndahl, K. Prydz, Overexpression of the 3′ -Phosphoadenosine 5′ -Phosphosulfate (PAPS) Transporter 1 Increases Sulfation of Chondroitin Sulfate in the Apical Pathway of MDCK II Cells, Glycobiology, 18 (2008) 53-65.

[11] K. Dejima, D. Murata, S. Mizuguchi, K.H. Nomura, T. Izumikawa, H. Kitagawa, K. Gengyo-Ando, S. Yoshina, T. Ichimiya, S. Nishihara, S. Mitani, K. Nomura, Two Golgi-resident 3′ -Phosphoadenosine 5′ -Phosphosulfate Transporters Play Distinct Roles in Heparan Sulfate Modifications and Embryonic and Larval Development in Caenorhabditis elegans, Journal of Biological Chemistry, 285 (2010) 24717-24728.

[12] S. Nishihara, Members of the Nucleotide-Sugar Transporter Family and Their Functions, in: Glycoscience: Biology and Medicine, Springer, 2015, pp. 1253-1265.

[13] M. Imamura, T. Kumagai, N. Sugihara, K. Furuno, High-Performance Liquid Chromatographic Assay of 3-Phosphoadenosine 5-Phosphosulfate (PAPS) and UDP-Glucuronic Acid (UDPGA) in Cultured Hepatic Cell Extracts, Journal of Health Science, 49 (2003) 395-400.

[14] M.R. Gama, R.G. da Costa Silva, C.H. Collins, C.B.G. Bottoli, Hydrophilic interaction chromatography, TrAC Trends in Analytical Chemistry, 37 (2012) 48-60.

[15] K.M. Jenkins, M.S. Young, C.R. Mallet, A.A. Elian, Mixed-mode solid-phase extraction procedures for the determination of MDMA and metabolites in urine using LC-MS, LC-UV, or GC-NPD, Journal of Analytical Toxicology, 28 (2004) 50-58.

[16] E. Brewer, J. Henion, Atmospheric pressure ionization LC/MS/MS techniques for drug disposition studies, Journal of Pharmaceutical Sciences, 87 (1998) 395-402.

[17] T. Uesugi, K. Sano, Y. Uesawa, Y. Ikegami, K. Mohri, Ion-pair reversed-phase high-performance liquid chromatography of adenine nucleotides and nucleoside using triethylamine as a counterion, Journal of Chromatography B: Biomedical Sciences and Applications, 703 (1997) 63-74.

[18] H. Chen, F.-m. Li, K.-l. Yang, X.-b. Li, H. Li, X. Wu, Determination of APS and PAPS by ion-pair reversed-phase phase high-performance liquid chromatography in liver of animals, Xinjiang Nongye Kexue, 51 (2014) 564-570.

[19] E. Lundanes, L. Reubsaet, T. Greibrokk, Chromatography: Basic Principles, Sample Preparations and Related Methods, Wiley-VCH, First Edition, 2012.

[20] G.A. Hazelton, J.J. Hjelle, R.L. Dills, C.D. Klaassen, A radiometric method for the measurement of adenosine 3'-phosphate 5'-phosphosulfate in rat and mouse liver, Drug Metabolism and Disposition: the biological fate of chemicals, 13 (1985) 30-34.

[21] K.O. Wong, K.P. Wong, Direct measurement and regulation of 3′-phosphoadenosine 5′-phosphosulfate (PAPS) generation in vitro, Biochemical Pharmacology, 52 (1996) 1187-1194.

[22] D.J. Sweeny, L.A. Reinke, Sulfation of acetaminophen in isolated rat hepatocytes. Relationship to sulfate ion concentrations and intracellular levels of 3'-phosphoadenosine-5'-phosphosulfate Drug Metabolism and Disposition, 16 (1988) 712-715.

[23] T.R. Pettitt, S.K. Dove, A. Lubben, S.D.J. Calaminus, M.J.O. Wakelam, Analysis of intact phosphoinositides in biological samples, Journal of Lipid Research, 47 (2006) 1588-1596.

[24] S. Banerjee, S. Mazumdar, Electrospray Ionization Mass Spectrometry: A Technique to Access the Information beyond the Molecular Weight of the Analyte International, Journal of Analytical Chemistry, 2012 (2012) 40.

[25] A. El-Aneed, A. Cohen, J. Banoub, Mass Spectrometry, Review of the Basics: Electrospray, MALDI, and Commonly Used Mass Analyzers, Applied Spectroscopy Reviews, 44 (2009) 210-230.

[26] P. Kebarle, U.H. Verkerk, Electrospray: From ions in solution to ions in the gas phase, what we know now, Mass Spectrometry Reviews, 28 (2009) 898-917.

[27] L.T. Cherney, Structure of Taylor cone-jets: limit of low flow rates, Journal of Fluid Mechanics, 378 (1999) 167-196.

[28] N.B. Cech, C.G. Enke, Practical implications of some recent studies in electrospray ionization fundamentals, Mass Spectrometry Reviews, 20 (2001) 362-387.

[29] E.C. Müller, Mass Spectrometry: ESI, in: Encyclopedic Reference of Genomics and Proteomics in Molecular Medicine, Springer Berlin Heidelberg, Berlin, Heidelberg, 2006, pp. 1020-1022.

[30] P.H. Dawson, ed. Quadrupole mass spectrometry and its applications, Elsevier, 2013.

[31] C. Colina-Coca, D. González-Peña, E. Vega, B. de Ancos, C. Sánchez-Moreno, Novel approach for the determination of volatile compounds in processed onion by headspace gas chromatography–mass spectrometry (HS GC–MS), Talanta, 103 (2013) 137-144.

[32] Y.R. Tahboub, M.F. Zaater, Z.A. Al-Talla, Determination of the limits of identification and quantitation of selected organochlorine and organophosphorous pesticide residues in surface water by full-scan gas chromatography/mass spectrometry, Journal of Chromatography A, 1098 (2005) 150-155.

[33] chromservis, GC/MS-TOF Description. https://www.chromservis.eu/i/gc-ms-tof-description?lang=EN, accessed 11.06.2016.

[34] openi, The path to clinical proteomics research: integration of proteomics, genomics, clinical laboratory and regulatory science. https://openi.nlm.nih.gov/detailedresult.php?img=PMC3116002_kjlm-31-61-g003&req=4, accessed 01.06.2016.

[35] J.-P. Antignac, K. de Wasch, F. Monteau, H. De Brabander, F. Andre, B. Le Bizec, The ion suppression phenomenon in liquid chromatography–mass spectrometry and its consequences in the field of residue analysis, Analytica Chimica Acta, 529 (2005) 129-136.

[36] T.M. Annesley, Ion Suppression in Mass Spectrometry, Clinical Chemistry, 49 (2003) 1041-1044.

[37] A.J.P. Martin, R.L.M. Synge, A new form of chromatogram employing two liquid phases: A theory of chromatography. 2. Application to the micro-determination of the higher monoamino-acids in proteins, Biochemical Journal, 35 (1941) 1358-1368.

[38] A. Zotou, An overview of recent advances in HPLC instrumentation, Central European Journal of Chemistry, 10 (2012) 554-569.

[39] J.J. Kirkland, J.W. Henderson, J.J. DeStefano, M.A. van Straten, H.A. Claessens, Stability of silica-based, endcapped columns with pH 7 and 11 mobile phases for reversed-phase high-performance liquid chromatography, Journal of Chromatography A, 762 (1997) 97-112.

[40] J.J. Kirkland, M.A. van Straten, H.A. Claessens, High pH mobile phase effects on silica-based reversed-phase high-performance liquid chromatographic columns, Journal of Chromatography A, 691 (1995) 3-19.

[41] J. Persson, P. Hemström, K. Irgum, Preparation of a sorbitol methacrylate grafted silica as stationary phase for hydrophilic interaction chromatography, Journal of Separation Science, 31 (2008) 1504-1510.

[42] B.A. Bidlingmeyer, F.V. Warren, Column efficiency measurement, Analytical Chemistry, 56 (1984) 1583A-1596A.

[43] B. Dejaegher, D. Mangelings, Y. Vander Heyden, Method development for HILIC assays, Journal of Separation Science, 31 (2008) 1438-1448.

[44] S. Fekete, J.-L. Veuthey, D. Guillarme, New trends in reversed-phase liquid chromatographic separations of therapeutic peptides and proteins: Theory and applications, Journal of Pharmaceutical and Biomedical Analysis, 69 (2012) 9-27.

[45] J.J. Kirkland, C.H. Dilks, J.J. DeStefano, Normal-phase high-performance liquid chromatography with highly purified porous silica microspheres, Journal of Chromatography A, 635 (1993) 19-30.

[46] L.R. Hutchings, S. Agostini, M.E. Oti, J. Keth, Normal-phase (temperature gradient) interaction chromatography – A powerful tool for the characterisation of high molecular weight chain-end functionalised polymers, European Polymer Journal, 73 (2015) 105-115.

[47] A. Williams, V. Frasca, Ion-Exchange Chromatography, in: Current Protocols in Protein Science, John Wiley & Sons, Inc., 2001.

[48] R. Oertel, V. Neumeister, W. Kirch, Hydrophilic interaction chromatography combined with tandem-mass spectrometry to determine six aminoglycosides in serum, Journal of Chromatography A, 1058 (2004) 197-201.

[49] P. Jandera, Stationary and mobile phases in hydrophilic interaction chromatography: a review, Analytica Chimica Acta, 692 (2011) 1-25.

[50] A.J. Alpert, Hydrophilic-interaction chromatography for the separation of peptides, nucleic acids and other polar compounds, Journal of Chromatography A, 499 (1990) 177-196.

[51] B. Buszewski, S. Noga, Hydrophilic interaction liquid chromatography (HILIC)—a powerful separation technique, Analytical and Bioanalytical Chemistry, 402 (2012) 231-247.

[52] M. Liu, J. Ostovic, E.X. Chen, N. Cauchon, Hydrophilic interaction liquid chromatography with alcohol as a weak eluent, Journal of Chromatography A, 1216 (2009) 2362-2370.

[53] P. Hemström, K. Irgum, Hydrophilic interaction chromatography, Journal of Separation Science, 29 (2006) 1784-1821.

[54] Z. Hao, B. Xiao, N. Weng, Impact of column temperature and mobile phase components on selectivity of hydrophilic interaction chromatography (HILIC), Journal of Separation Science, 31 (2008) 1449-1464.

[55] MerckMillipore, Hydrophilic Interaction Liquid Chromatography. https://www.merckmillipore.com/NO/en/analytics-and-sample-preparation/sequant/what-is-hilic/Ih2b.qB.xfgAAAFFw6IcWdZp,nav?bd=1, accessed 01.06.2016.

[56] F. Riedo, E.s. Kováts, Adsorption from liquid mixtures and liquid chromatography, Journal of Chromatography A, 239 (1982) 1-28.

[57] Z. Lü, P. Zhang, L. Jia, Preparation of chitosan functionalized monolithic silica column for hydrophilic interaction liquid chromatography, Journal of Chromatography A, 1217 (2010) 4958-4964.

[58] B.W. Pack, D.S. Risley, Evaluation of a monolithic silica column operated in the hydrophilic interaction chromatography mode with evaporative light scattering

detection for the separation and detection of counter-ions, Journal of Chromatography A, 1073 (2005) 269-275.

[59] A. Berthod, H.L. Jin, T.E. Beesley, J.D. Duncan, D.W. Armstrong, Cyclodextrin chiral stationary phases for liquid chromatographic separations of drug stereoisomers, Journal of Pharmaceutical and Biomedical Analysis, 8 (1990) 123-130.

[60] T. Ikegami, K. Tomomatsu, H. Takubo, K. Horie, N. Tanaka, Separation efficiencies in hydrophilic interaction chromatography, Journal of Chromatography A, 1184 (2008) 474-503.

[61] Y. Xuan, E.B. Scheuermann, A.R. Meda, H. Hayen, N. von Wirén, G. Weber, Separation and identification of phytosiderophores and their metal complexes in plants by zwitterionic hydrophilic interaction liquid chromatography coupled to electrospray ionization mass spectrometry, Journal of Chromatography A, 1136 (2006) 73-81.

[62] SeQuant, A Practical Guide to HILIC. http://www.google.no/url?sa=t&rct=j&q=&esrc=s&source=web&cd=1&cad=rja&uact=8&ved=0ahUKEwizlaCErqnMAhWGEywKHT2hB_EQFggbMAA&url=http%3A%2F%2Fwww.hplc.eu%2FDownloads%2FMerckSeQuant_ZIC_HILIC_Guide.pdf&usg=AFQjCNFcUsj5gkacbjxFNXcp1Vl4pG5v4g&sig2=nDvW_kjyEFh4yEoLTyaeXg&bvm=bv.119745492,d.bGg, accessed 25.04.2016.

[63] E. Johnsen, Hydrophilic interaction chromatographic separation of 8 deoxynucleotide triphosphates (dNTPs) and nucleotide triphosphates (NTPs), thesis, 2010.

[64] Y. Guo, S. Gaiki, Retention behavior of small polar compounds on polar stationary phases in hydrophilic interaction chromatography, Journal of Chromatography A, 1074 (2005) 71-80.

[65] E. Johnsen, S.R. Wilson, I. Odsbu, A. Krapp, H. Malerod, K. Skarstad, E. Lundanes, Hydrophilic interaction chromatography of nucleoside triphosphates with temperature as a separation parameter, Journal of Chromatography A, 1218 (2011) 5981-5986.

[66] J. Chen, W. Wang, S. Lv, P. Yin, X. Zhao, X. Lu, F. Zhang, G. Xu, Metabonomics study of liver cancer based on ultra performance liquid chromatography coupled to mass spectrometry with HILIC and RPLC separations, Analytica Chimica Acta, 650 (2009) 3-9.

[67] M. Sergi, C. Montesano, S. Napoletano, D. Pizzoni, C. Manetti, F. Colistro, R. Curini, D. Compagnone, Analysis of Bile Acids Profile in Human Serum by Ultrafiltration Clean-up and LC-MS/MS, Chromatographia, 75 (2012) 479-489.

[68] G. Shen, H.K. Lee, Hollow Fiber-Protected Liquid-Phase Microextraction of Triazine Herbicides, Analytical Chemistry, 74 (2002) 648-654.

[69] A.E. Hagerman, Radial diffusion method for determining tannin in plant extracts, Journal of Chemical Ecology, 13 (1987) 437-449.

[70] K. Inoue, E. Yamada, T. Hino, H. Oka, Hydrophilic Interaction Liquid Chromatography Tandem Mass Spectrometry Method for the Determination of Bicozamycin in Milk, Journal of Liquid Chromatography & Related Technologies, 32 (2009) 1914-1924.

[71] K. Inoue, S. Nitta, T. Hino, H. Oka, LC-MS/MS and centrifugal ultrafiltration method for the determination of novobiocin in chicken, fish tissues, milk and human serum, Journal of Chromatography B, 877 (2009) 461-464.

[72] K. Kishida, Simplified extraction of tetracycline antibiotics from milk using a centrifugal ultrafiltration device, Food Chemistry, 126 (2011) 687-690.

[73] E. Johnsen, O.K. Brandtzaeg, T. Vehus, H. Roberg-Larsen, V. Bogoeva, O. Ademi, J. Hildahl, E. Lundanes, S.R. Wilson, A critical evaluation of Amicon Ultra centrifugal filters for separating proteins, drugs and nanoparticles in biosamples, Journal of Pharmaceutical and Biomedical Analysis, 120 (2016) 106-111.

[74] MerckMillipore, Amicon Ultra-0.5 mL Centrifugal Filters for DNA and Protein Purification and Concentration. https://www.merckmillipore.com/NO/en/product/Amicon-Ultra-0.5%C2%A0mL-Centrifugal-Filters-for-DNA-and-Protein-Purification-and-Concentration,MM_NF-C82301?bd=1, accessed 29.05.2016.

[75] MerckMillipore, Water in the Laboratory. http://www.merckmillipore.com/NO/en/water-purification/learning-centers/tutorial/grades/eSqb.qB.3lUAAAFAcqlkiQz8,nav, accessed 19.05.2016.

[76] Sigma-Aldrich, Adenosine 3′ -phosphate 5′ -phosphosulfate lithium salt hydrate. http://www.sigmaaldrich.com/catalog/product/sigma/a1651?lang=en&region=NO, accessed 19.05.2016.

[77] X. Zhou, K. Chandarajoti, T.Q. Pham, R. Liu, J. Liu, Expression of heparan sulfate sulfotransferases in Kluyveromyces lactis and preparation of 3′ -phosphoadenosine-5′ -phosphosulfate, Glycobiology, 21 (2011) 771-780.

[78] M.D. Burkart, M. Izumi, E. Chapman, C.-H. Lin, C.-H. Wong, Regeneration of PAPS for the enzymatic synthesis of sulfated oligosaccharides, The Journal of Organic Chemistry, 65 (2000) 5565-5574.

[79] MerckMillipore, Amicon Ultra-0.5 Centrifugal Filter Unit with Ultracel-10 membrane. http://www.merckmillipore.com/NO/en/product/Amicon-Ultra-0.5-Centrifugal-Filter-Unit-with-Ultracel-10-membrane,MM_NF-UFC501096, accessed 19.05.2016.

[80] MerckMillipore, SeQuant® ZIC®-pHILIC 5µm polymer 150 x 2.1 mm. http://www.merckmillipore.com/NO/en/product/SeQuant-ZIC-pHILIC-5%C2%B5m-polymer-150-x-2.1-mm,MDA_CHEM-150460, accessed 19.05.2016.

[81] B. Chauve, D. Guillarme, P. Cléon, J.L. Veuthey, Evaluation of various HILIC materials for the fast separation of polar compounds, Journal of Separation Science, 33 (2010) 752-764.

[82] C.S. Grumbach, Hydrophilic interaction chromatography using silica columns for the retention of polar analytes and enhanced ESI-MS sensitivity, LC GC North America, 22 (2004) 1010.

[83] R.C. Castells, C.B. Castells, M.A. Castillo, Influence of differences between sample and mobile phase viscosities on the shape of chromatographic elution profiles, Journal of Chromatography A, 775 (1997) 73-79.

[84] M.A. Strege, Hydrophilic interaction chromatography-electrospray mass spectrometry analysis of polar compounds for natural product drug discovery, Analytical Chemistry, 70 (1998) 2439-2445.

[85] Scifinder, PAPS. https://scifinder.cas.org/scifinder/view/scifinder/scifinderExplore.jsf, accessed 08.06.2016.

[86] G. Greco, T. Letzel, J Main Interactions and Influences of the Chromatographic Parameters in HILIC Separations, Journal of Chromatographic Science, 51 (2013) 684-693.

[87] H.G. Gika, G.A. Theodoridis, R.S. Plumb, I.D. Wilson, Current practice of liquid chromatography–mass spectrometry in metabolomics and metabonomics, Journal of Pharmaceutical and Biomedical Analysis, 87 (2014) 12-25.

[88] bio-protocol, Enrichment of Golgi membranes from HeLa cells by sucrose gradient ultracentrifugation. http://www.bio-protocol.org/e906, accessed 31.05.2016.

[89] P. De Bièvre, H. Günzler, Validation in chemical measurement, Springer, First Edition, 2005.

[90] P.A. Baeuerle, W.B. Huttner, Chlorate—a potent inhibitor of protein sulfation in intact cells, Biochemical and Biophysical Research Communications, 141 (1986) 870-877.

[91] K. Fjeldstad, M.E. Pedersen, T.T. Vuong, S.O. Kolset, L.M. Nordstrand, K. Prydz, Sulfation in the Golgi lumen of Madin-Darby canine kidney cells is inhibited by brefeldin A and depends on a factor present in the cytoplasm and on Golgi membranes, Journal of Biological Chemistry, 277 (2002) 36272-36279.

[92] G. Mitulovic, C. Stingl, I. Steinmacher, O. Hudecz, J.R. Hutchins, J.-M. Peters, K. Mechtler, Preventing carryover of peptides and proteins in nano LC-MS separations, Analytical Chemistry, 81 (2009) 5955-5960.

[93] D.A. Herzlinger, T.G. Easton, G.K. Ojakian, The MDCK epithelial cell line expresses a cell surface antigen of the kidney distal tubule, The Journal of Cell Biology, 93 (1982) 269-277.

[94] A. Wandinger-Ness, M.K. Bennett, C. Antony, K. Simons, Distinct transport vesicles mediate the delivery of plasma membrane proteins to the apical and basolateral domains of MDCK cells, The Journal of Cell Biology, 111 (1990) 987-1000.

[95] R. Bacallao, C. Antony, C. Dotti, E. Karsenti, E. Stelzer, K. Simons, The subcellular organization of Madin-Darby canine kidney cells during the formation of a polarized epithelium, The Journal of Cell Biology, 109 (1989) 2817-2832.

[96] O. Tacar, P. Sriamornsak, C.R. Dass, Doxorubicin: an update on anticancer molecular action, toxicity and novel drug delivery systems, Journal of Pharmacy and Pharmacology, 65 (2013) 157-170.

[97] H.C. Dippold, M.M. Ng, S.E. Farber-Katz, S.-K. Lee, M.L. Kerr, M.C. Peterman, R. Sim, P.A. Wiharto, K.A. Galbraith, S. Madhavarapu, GOLPH3 bridges phosphatidylinositol-4-phosphate and actomyosin to stretch and shape the Golgi to promote budding, Cell, 139 (2009) 337-351.

[98] B. Liu, J.-W. Jiang, B.C. Wilson, L. Du, S.-N. Yang, J.-Y. Wang, G.-C. Wu, X.-D. Cao, J.-S. Hong, Systemic infusion of naloxone reduces degeneration of rat substantia nigral dopaminergic neurons induced by intranigral injection of lipopolysaccharide, Journal of Pharmacology and Experimental Therapeutics, 295 (2000) 125-132.

6 Appendix

6.1 Preparation and purification of the internal standard (^{13}C-PAPS)

This section was performed by Kristian Prydz (Professor at the Section for Physiology and Cell Biology, Department of Biosciences, UiO). The procedure that was used for preparation and purification of ^{13}C-PAPS was similar to the procedure used for preparation and the purification of PAPS (described in this section). ATP 13C-10 from Sigma Aldrich was used.

PAPS synthesis is presented in **Figure 4**. Sodium sulfate and adenosine 5'- triphosphate (ATP) are first converted to adenosine 5'-phosphosulfate (APS), and then the second phospho group is added to produce PAPS. PPi represents pyrophosphate, and Pi represents phosphate.

6.1.1 Sample induction protocol

An induction protocol for a 25 ml culture of pET-Duet-1 or pCDF-Duet-1 in E. coli BL21 Star (DE3) is described here. The enzymes involved in synthesizing PAPS, including ATP sulfurylase, APS kinase and pyrophosphatase, were expressed in E. coli BL21 Star (DE3) (Invitrogen). ATP sulfurylase and APS kinase were expressed by KAST-APSK-pETDuet-1, ampicillin resistance. Pyrophosphatase was expressed by PPA-pCDFDuet-1, streptomycin resistance.

- Inoculated a clone, from fresh plate prepared from stock bacteria the day before, with 25 ml overnight Express Instant TB autoinduction medium with antibiotics (50 µg/ml ampicillin or streptomycin) in a 125 ml culture flask. Left bacteria at 28 degrees shaking at 300 rpm overnight.
- Harvested bacteria the day after by centrifugation at 4000xg for 15 min, 17 hours inoculation. 0.872 g wet weight for PPA and 0.874 g wet weight for KAST.
- Lysed cells with sonication in 20 mM Tris, 500 mM NaCl, pH 7.8. Added 10 % glycerol. A total volume of ~13 mL.
- Protein concentration according to BCA:

a. PPA: 1.78 mg/mL, concentrated to 16.6 mg/mL.
b. KAST-APSK: 1.28 mg/mL, concentrated to 29.8 mg/mL.

6.1.2 PAPS synthesis

The PAPS preparation was achieved by crude enzymes. The reaction buffer included:

- 50 mM Tris–HCl at pH 8.0 with 100 mM Na_2SO_4, 10 mM $MgCl_2$, 10 mM LiCl
- 5 mM ATP disodium salt hydrate (Sigma A2383, 551.14 g/mol)
- 0.6 mg/mL of crude ATP sulfurylase and APS kinase (29.8 mg/ml)
- 0.15 mg/mL of crude pyrophosphatase (16.6 mg/ml)

The conversion was quantitative after 70 min, with ~60% PAPS, ~10% ADP and ~30 % AMP, as determined by HPLC on an Amide-80 HILIC column.

The reaction mixture was filtered through a 0.45 μm membrane and loaded onto a 5 ml DEAE FF (GE Life Sciences) prepacked column. The column was washed with ~10 column volumes of 50 mM NaCl and eluted with a 20 column volume gradient from 50-1000 mM NaCl at ~3.5 mL/min. E^{mM}=15.4 for PAPS at 259 nm and pH 7.0.

6.2 Preparation of the samples

This section was performed by Ravi Adusumalli (PhD student at the Section for Physiology and Cell Biology, Department of Biosciences, UiO).

6.2.1 Cell culture work

Adherent Madin-Darby canine kidney epithelial (MDCK) cells represent the model of this thesis. The MDCK II cell line is mostly used to perform the studies of polarized epithelia; it is one of two subclones of the original cell line obtained from dog kidney [93-95]. After stable transfection and clonal selection, several cell strains that display different recombinant proteins have been determined within the research group (**Table 7**).

Cells were protected in an incubator at 37 °C with 5 % CO_2 in the incubator atmosphere, and the cell culturing process was conducted in a laminar cell culture hood in a designated cell lab. In order to preserve MDCK cells, cells were grown

under specific conditions in 75 cm^2 flasks with ventilated caps containing 20 ml of complete growth medium consisted of Dulbeccos's modified Eagle's Medium (DMEM), containing 5 % fetal calf serum (FCS) and (1 %) penicillin/streptomycin (P/S).

Table 7: List of MDCK cell lines that will be used in this thesis.

Cell Line	Description
MDCK I	Cells from later passages of MDCK.
MDCK II	Cells from later passages of MDCK.
MDCK II B10	MDCK II cells stably expressing PAPST1-GFP.
MDCK II B2	MDCK II cells stably expressing PAPST1-GFP.
MDCK II PAPST1-GFP (B22)	MDCK II cells stably expressing PAPST1-GFP.

Expansion of cells: Trypsination of MDCK II cells grown in 75 cm^2 flasks

Adherent MDCK II cells have gradually increased to reach the level of confluency in 75 cm^2 flasks; therefore, confluent epithelial cell layers were transferred to new flasks to provide suitable growing conditions that ensure the continuous dividing during the exponential phase of the growth cycle. Ethylenediaminetetraacetic acid (EDTA) was used to create gaps in the tight monolayer to facilitate the diffusion of Trypsin through the layers and the degradation of proteins, that support cells to adhere to the flask, in the basolateral domain.

Protocol:

- Remove medium from the bottle.
- Wash cells with 10 mL Phosphate-buffered saline (PBS) containing EDTA.
- Add 5 mL Trypsin-EDTA to each bottle. Remove after 3-5 min, or when cells are beginning to round up.
- Add 2 mL Trypsin-EDTA and leave the cells in incubator for 10-15 min, or until all the cells have detached.
- Add 10 mL of complete growth medium to the flask, and resuspend the cells.
- Transfer cells to new bottles. If transferring to new 75 cm^2 flasks, then transfer 2 mL of the cell suspension to each flask containing 20 mL of fresh complete growth medium.

6.2.2 Cell viability assays

To prove this thesis, cells were killed or had apoptosis because of the intentional use of chemical destructive agents in high concentrations that had a potential to ruin the DNA [96-98]. Another important matter was considered is the use of whole populations of cells grown in a dish or on a filter in order to determine the cell viability assay, which was required to ensure the suitable and reproducible conditions for the biochemical experiments.

Trypan blue stain

To conduct the cell viability assay, Trypan blue exclusion test was performed. Trypan blue works on penetrating the broken permeable membranes in the dead cells and colouring the interior of cells in a blue colour while it is not able to do that for viable cells that will appear as a solid non-blue core. Then, by a manual or automatic counting under a microscope, the number of living cells will be determined. CountessTM automated cell counter was used for this experiment.

Protocol:

- Wash cells with 1 mL of PBS with EDTA.
- Add 0.5 mL of Trypsin-EDTA.
- Incubate for 15 min, or until all cells have detached from the substratum.
- Add 2 mL of cell growth medium, then transfer to centrifugal tubes.
- Centrifuge at 1500 rpm for 5 min.
- Remove supernatant and resuspend pellet in 1mL of cell growth medium
- Add 10 µL of the cell suspension to a new tube.
- Add 10 µL of Trypan blue (0.4 %) and mix well by pipetting.
- Remove 20 µL of Trypan blue stained cell suspension and add to Countess™ cell counter slide.
- Insert slide into Countess™, focus the counter properly (live cells have a bright center, dead cells have a dark center) and count the cells.

Solutions:

10 x PBS: 2.62 g NaH2PO4 x H2O, 14.42 g NaH2PO4 x 2H2O, 87.66 g NaCl. Mix NaH2PO4 x H2O and NaH2PO4 x 2H2O with 300 mL dH2O while stirring. Add NaCl stepwise. At the end, add dH2O to 1 L. Adjust pH to 7.4 before autoclaving.

10 x PBS with EDTA: 2.62g NaH2PO4 x H2O, 14.42 g NaH2PO4 x 2H2O, 87.66 g NaCl and 18.64 g EDTA. Mix NaH2PO4 x H2O and NaH2PO4 x 2H2O with 300 mL dH2O while stirring. Add NaCl stepwise, then EDTA. At the end, add dH2O to 1 L. Adjust pH to 7.4 before autoclaving.

Making Cell pellets for PAPS quantification:

After the confluence of the cell lines of MDCK I, MDCK II, B22, B10, and B2, each cell line was divided into 6 different T 75cm^2 flasks. When the cells reach confluence, the old medium was removed and cells washed one time with 20 mL of serum-free DMEM with glutamate. More additions of serum-free DMEM with glutamate were performed and flasks were incubated for one hour. At the end of the incubation process, flasks were washed with a serum-free medium one time only.

Three flasks washed one time with 5 mL trypsin for 5 minutes. Then, the old medium was removed and added fresh 2 mL of trypsin for cells to detach them. Later, serum-free medium was added to dilute the medium and the solution was centrifuged for 5 minutes at low rpm. The supernatant was discarded and the pellet was diluted with 14 mL of PBS-EDTA.

The other three flasks of each group were washed one time with 10 mL of cold PBS with EDTA. To perform cells scraping, 10 mL of the same PBS with EDTA was replaced. Then Rinse with additional 4 mL of PBS-EDTA was done. Solutions were transferred into 15 mL centrifuge tubes and centrifuged for 5 minutes. Supernatant removed and new 10 mL of PBS-EDTA added, and again another one round of centrifugation was conducted. The process of washing was repeated and supernatant removed. MDCK I, II, B22, B10 and B2 pellets stored at -80 °C.

6.2.3 Isolation of Golgi vesicles

Golgi fraction was isolated by sucrose gradient method. The cells were scraped and collected into 50 mL falcon tubes and centrifuged at 1000 rpm, 12 °C for 5 minutes. The cell pellets were diluted with 2 mL homogenisation buffer. The cell suspension was squeezed by using 22 G syringe and centrifuged at 2600 rpm for 10 minutes. The supernatant was collected and the pellets were diluted with 2 mL homogenisation buffer. This was repeated 1-2 times. Collected post-nuclear supernatant (PNS)

solution was transferred to a 15 mL Falcon tube and diluted with homogenisation buffer to 8.4 mL. 6.6 mL of 2 M sucrose was added to a total volume of 15 mL. The gradient tube was placed in SW 32 swing-out rotor and centrifuged at 28000 rpm, 4 °C for 4.20 hours. The white portion of the upper and lower bands was transferred into labelled tubes. The upper and lower bands were diluted with 1X PBS, and placed in MLA 80 fixed angel rotor. The tubes were centrifuged at 50000 rpm, 4 °C for 1 hour. The supernatant was discarded. The gel (like pellets) was diluted with 1X PBS, transferred to Eppendorf tube and centrifuged at maximum speed by using bench top ultracentrifuge. The pellets were collected, 200 µL of 1X PBS was added. The tubes were stored at -80 °C for HPLC analysis.

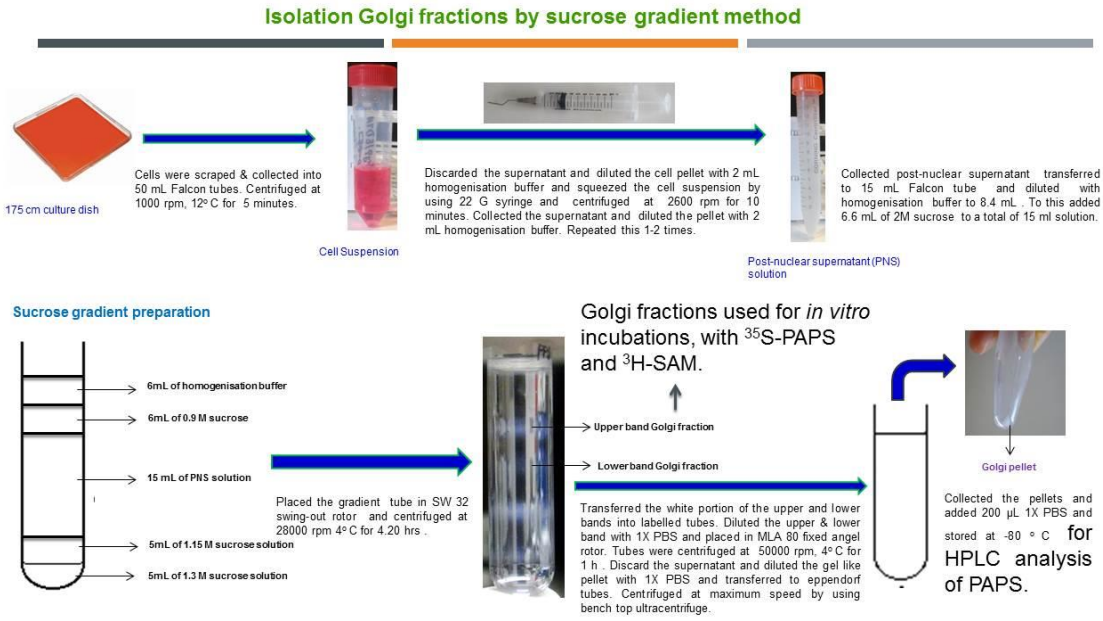

Figure 39: Isolation of Golgi fraction. The figure was provided by Ravi Adusumalli (PhD student at the Section for Physiology and Cell Biology, Department of Biosciences, UiO).

6.3 Linearity in the mobile phases

The linearity was investigated in mobile phases that were used during the optimization of the method. All mobile phases show good linearity ($R^2 > 0.99$).

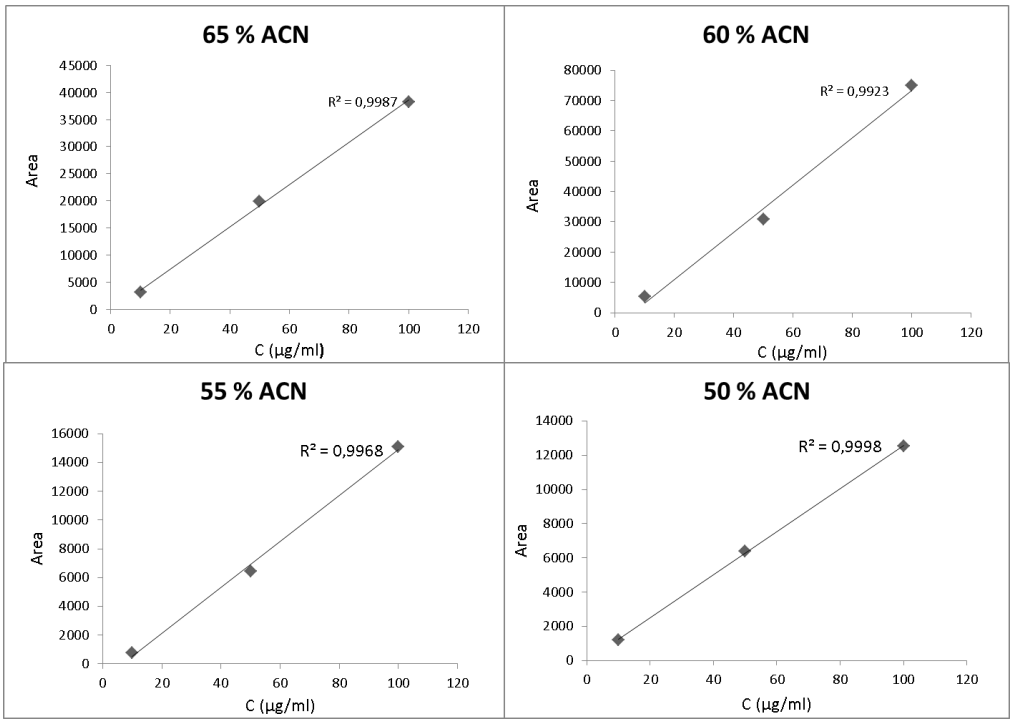

Figure 40: Linearity of the mobile phases. PAPS standard solutions of 10, 50 and 100 µg/mL were used with mobile phases contain 50, 55, 60 and 65 % ACN in the mobile phase. Other chromatographic conditions were as described in **Figure 16**.

6.4 Variation in the retention time with 70 % ACN in the MP

A variation in the retention time when 70 % ACN was used in the mobile phase was observed during the optimizing of the method (**Figure 41**).

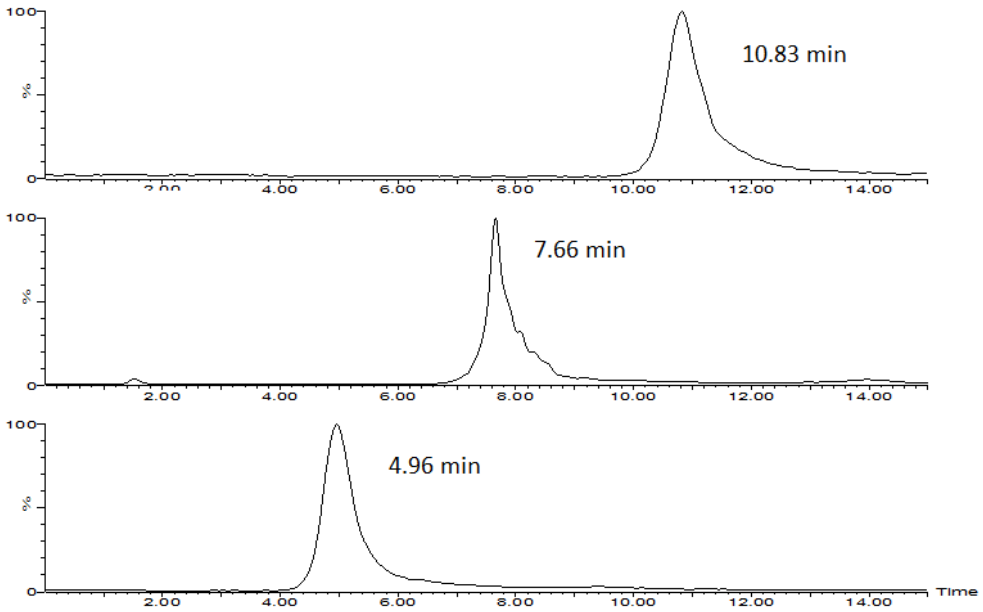

Figure 41: Retention time variation. Chromatograms of 100 µg/mL standard solutions, the mobile phase consisted of ACN/100 mM $(NH_4)_2CO_3$ (70/30, v/v). The chromatographic conditions are described in **Figure 16**.

6.5 ESI-MS spectra of IS

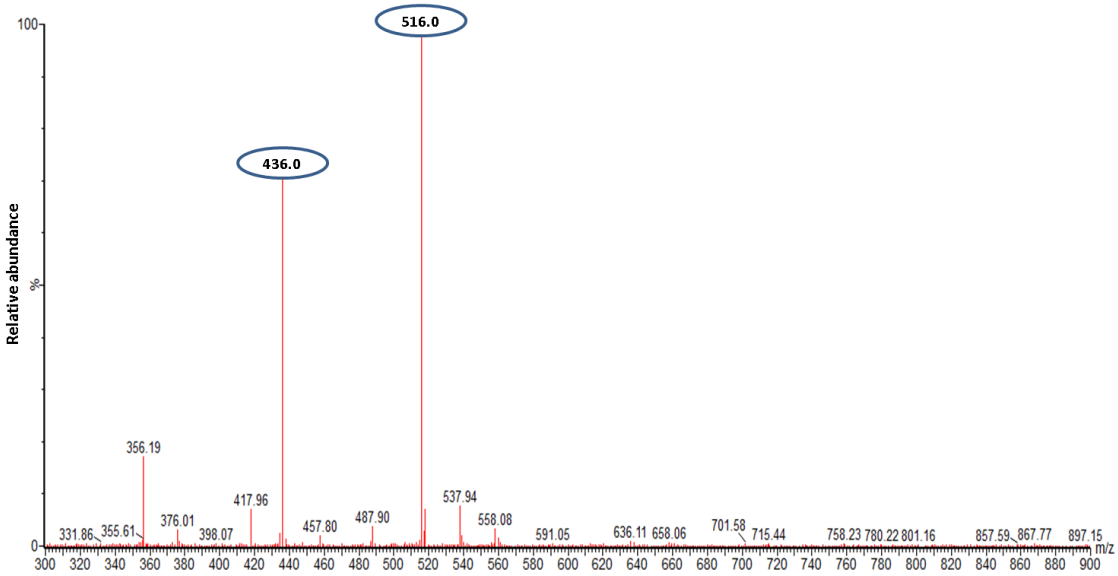

Figure 42: ESI-MS of 100 µg/mL standard solution of the internal standard. Direct injection, negative mode, and full scan data acquisition in range of *m/z* 300 – 900.

6.6 Evaluation calculations

6.6.1 Between replicates and between day repeatability

Table 8 and Table 9 shows data used to calculate repeatability between replicates (n=6) and repeatability between days (n=5), respectively.

Table 8: Between replicate repeatability calculations.

Concentration µg/mL	**2**	**10**	**100**	**200**
Replicate	A/A_{IS}	A/A_{IS}	A/A_{IS}	A/A_{IS}
1	0,1934	0,7885	9,4142	18,0848
2	0,1849	0,7541	13,4148	19,7043
3	0,1788	0,7242	10,5275	18,7106
4	0,2440	0,8561	10,9881	20,5591
5	0,1874	0,8111	11,1532	21,6910
6	0,1504	1,1636	8,5254	18,6344
Average	0,1898	0,8496	10,6705	19,5641
STDEV	0,0305	0,1604	1,6772	1,3649
RSD (%)	16,0757	18,8831	15,7181	6,9764

Table 9: Between day repeatability calculations.

Concentration µg/mL	**2**	**10**	**100**	**200**
Day	A/A_{IS}	A/A_{IS}	A/A_{IS}	A/A_{IS}
1	0,1857	0,8186	10,2222	18,8333
2	0,1044	0,9304	9,8647	17,8020
3	0,1501	1,2269	10,4104	18,4412
4	0,1728	0,9652	9,5619	17,1135
5	0,1558	1,0448	9,6224	17,2889
Average	0,1538	0,9972	9,9363	17,8958
STDEV	0,0310	0,1520	0,3709	0,7358
RSD (%)	20,1568	15,2421	3,7331	4,1114